Freie Universität Berlin

Department of Earth Sciences

Institute of Geological Sciences

Sediment-biogeochemical characterization of a thermokarst lake basin in Central Alaska

Bachelor Thesis

by

Filip Matuszewski

Supervisors:

Prof. Dr. Anne Bernhardt,

Free University Berlin, Institute of Geological Sciences

Dr. Josefine Lenz,

Alfred Wegener Institute, Helmholtz Centre for Polar and Marine Research

and University of Alaska Fairbanks

November 28, 2017

Eidesstattliche Erklärung zur Bachelorarbeit

Ich, Filip Matuszewski (Matr.-Nr.: 4786276), versichere, die Bachelorarbeit selbständig und lediglich unter Benutzung der angegebenen Quellen und Hilfsmittel verfasst zu haben.

Ich erkläre weiterhin, dass die vorliegende Arbeit noch nicht im Rahmen eines anderen Prüfungsverfahrens eingereicht wurde.

Berlin, den

_____
(Unterschrift)

Abstract

When permafrost is thawing, the excess water forms so called thermokarst lakes which are very dynamic systems. In this thesis, the depositional environment of a thermokarst lake in discontinuous permafrost is characterized sedimentological and biogeochemical using four sediment cores from Goldstream Lake in Central Alaska to test the hypotheses:

1) Near-shore deposits are characterized by a coarser grain size distribution, larger minerogenic input from terrestrial origin and a mixed source of lacustrine and terrestrial organic matter whereas central lake deposits are finer grained and contain less organic matter from terrestrial origin than near-shore sediments.

2) A longer sediment record from the lake center potentially preserves pre-lake deposits which are indicated by terrestrial organic matter and low organic carbon content due to microbial decomposition in the talik. Low decomposed, terrestrial peat indicates the lake on-set and is followed by a lacustrine phase.

Grain size analysis, magnetic susceptibility, total carbon, total nitrogen, total organic carbon and stable carbon isotopes were used to describe the differences between near-shore and central sediments. Furthermore, the biogeochemical methods were used to describe the sedimentary succession by distinguishing between present lake sediments with lacustrine organics and wetland peat underlaid by pre-lake sediments with terrestrial organics. The results show that central lake sediments are characterized by smaller grain sizes, less minerogenic input of terrestrial origin and a more organic matter from lacustrine origin than near-shore sediments. While present lake sediments and the wetland peat layer show the expected origin of organic matter, the pre-lake sediments indicate an older lake generation preserved below the terrestrial drainage peat.

Zusammenfassung

Wenn Permafrost auftaut, bildet das überschüssige Wasser so genannte thermokarst Seen, die sehr dynamische Systeme sind. In dieser Arbeit wird das Ablagerungsmilieu eines Thermokarstsees im diskontinuierlichem Permafrost sedimentologisch und biogeochemisch mit vier Sedimentkernen aus dem Goldstream Lake in Zentral-Alaska charakterisiert, um die folgenden Hypothesen zu testen:

1) Ufernahe Sedimente zeichnen sich durch eine gröbere Korngrößenverteilung, einem größeren mineralogenen Input aus terrestrischem Ursprung und einer gemischten Quelle von lakustriner und terrestrischer organischer Materie aus, während zentrale Seesedimente feinkörniger sind und weniger organische Materie terrestrischen Ursprungs enthalten als ufernahe Sedimente.

2) Längerer Sedimentkerne aus dem Zentrum des Sees bewahren möglicherweise Vorseesedimente, die durch terrestrische organische Materie und einen geringen organischen Kohlenstoffgehalt aufgrund mikrobieller Zersetzung im Talik angezeigt werden. Ein schlecht zersetzter, terrestrischer Torf weist auf den Anfang des Sees hin, gefolgt von einer lakustrinen Phase.

Korngrößenanalyse, die magnetischen Suszeptibilität, der Gesamtkohlenstoff, Gesamtstickstoff, organischer Kohlenstoff und stabile Kohlenstoffisotope wurden verwendet, um die Unterschiede zwischen ufernahen und zentralen Seesedimenten zu beschreiben. Darüber hinaus wurden die biogeochemischen Methoden zur Beschreibung der Sedimentabfolge verwendet, indem zwischen heutigen Seesedimenten mit lakustriner organischer Materie und Torf mit unterliegendem Vorseesedimenten mit terrestrischen organischen Stoffen unterschieden wurde. Die Ergebnisse zeigen, dass zentrale Seesedimente kleinere Korngrößen, weniger minerogenen Eintrag terrestrischen Ursprungs und mehr organische Materie lakustriner Herkunft aufweisen als ufernahe Sedimente. Während die vorhandenen Seesedimente und die Torfschicht die erwartete Herkunft der organischen Materie aufweisen, weisen die Vorseesedimente auf eine ältere Seegeneration hin, die unter dem Torf erhalten geblieben sind.

Contents

Figures

Tables

1. Introduction

1.1 Scientific relevance and background

The human-induced increase of greenhouse gases in the Atmosphere is known to accelerate climate change. The effects of climate change are particularly noticeable in the Arctic. Major parts of Alaska, Canada and Siberia are dominated by permafrost (Fig. 1) which is described as ground, that is frozen continuously under 0°C for at least two consecutive years (Van Everdingen, 2005).

Figure 1: Circumpolar map of permafrost distribution (Brown et al. 1998, *data from International Permafrost Association, 1998. Circumpolar Active-Layer Permafrost System (CAPS), version 1.0.)*

Approximately 22.79 x 10^6 km² or 23.9% of the exposed land area in the Northern Hemisphere is classified as permafrost region (Zhang et al., 1999). However, the percentage of actual permafrost in discontinuous, sporadic and isolated permafrost regions varies between 0 and 90%. Approximately 12.21 to 16.98 x 10^6 km², or 12.8% to 17.8% of the exposed land area in the Northern Hemisphere are treated actual permafrost (Zhang et al., 2000). Permafrost is considered one of the largest reservoirs of carbon. Rising annual temperatures due to climate change cause permafrost thaw and degradation which leads

to the formation of thermokarst lakes and the release of harmful greenhouse gases. Thermokarst lakes are considered 1) sources of atmospheric greenhouse gases like methane and carbon dioxide (Walter et al., 2006, Walter et al., 2007, Petrenko et al., 2009, Brosius et al., 2012) and 2) sinks in which organic carbon accumulates (Schirrmeister et al., 2011). The unfrozen area beneath a thermokarst lake, known as the talik, which forms due to a local anomaly in thermal, hydrological, hydrogeological, or hydrochemical conditions (Van Everdingen, 2005). The formation of taliks can lead to the mobilization of freshly thawed organic carbon from virgin yedoma (Kessler et al., 2012). The highest rates of CH4 emissions occur during methanogenesis at actively expanding taliks along thermokarst margins (Walter et al., 2006).

Therefore, the study and research on thermokarst lakes is very important to better understand the consequences and effects of thawing permafrost and the formation of thermokarst lakes on the climate change in the Arctic.

1.2 Research Hypothesis

The dynamic evolution of thermokarst lakes is derived from the physical and chemical sediment properties. The aim of this study is to characterize the lake-internal depositional environment by describing four sediment cores of Goldstream Lake with sedimentological and biogeochemical methods.

The research hypotheses are:

1) Near-shore deposits are characterized by a coarser grain size distribution, larger minerogenic input from terrestrial origin and a mixed source of lacustrine and terrestrial organic matter whereas central lake deposits are finer grained and contain less organic matter from terrestrial origin than near-shore sediments.

2) A longer sediment record from the lake center potentially preserves pre-lake deposits which are indicated by terrestrial organic matter and low organic carbon content due to microbial decomposition in the talik. Low decomposed, terrestrial peat indicates the lake on-set and is followed by a lacustrine phase.

2. Geographical and geological background

2.1 Quaternary Geology

Quaternary deposits are dominated by eolian sediments in Alaska. Loess which is described as homogenous, non-layered, porous and predominantly silt-sized sediment (Leonhard, 1823), can be found almost everywhere below altitudes of 300-450 m and forms the thickest layers in central and western Alaska. Thicknesses reach from a few millimeters to 60 m with recent accumulation rates of 0.2-2 mm per year (Péwé, 1975). Vulcanic deposits are also locally present in southern and western Alaska and are recorded, in drained lake basins (Lenz et al., 2016a). Glacial deposits are widely present in Alaska as large parts of North and South Alaska were covered by quaternary glaciers whereas Central Alaska remained ice-free (Péwé, 1975).

Alaska features different types of permafrost (Fig. 2). North Alaska is dominated by continuous permafrost which is described as a geographical region where permafrost is present everywhere beneath the exposed land surface. (Van Everdingen, 2005). Central Alaska indicates large areas of discontinuous permafrost which is described as a region where 50-90% of the exposed land surface is dominated by permafrost. Sporadic and isolated permafrost is present in South Alaska and describes a permafrost distribution below 50%. The distribution of permafrost across Alaska is clearly influenced by the temperature of different latitudes. Goldstream Lake is located in the area of discontinuous permafrost.
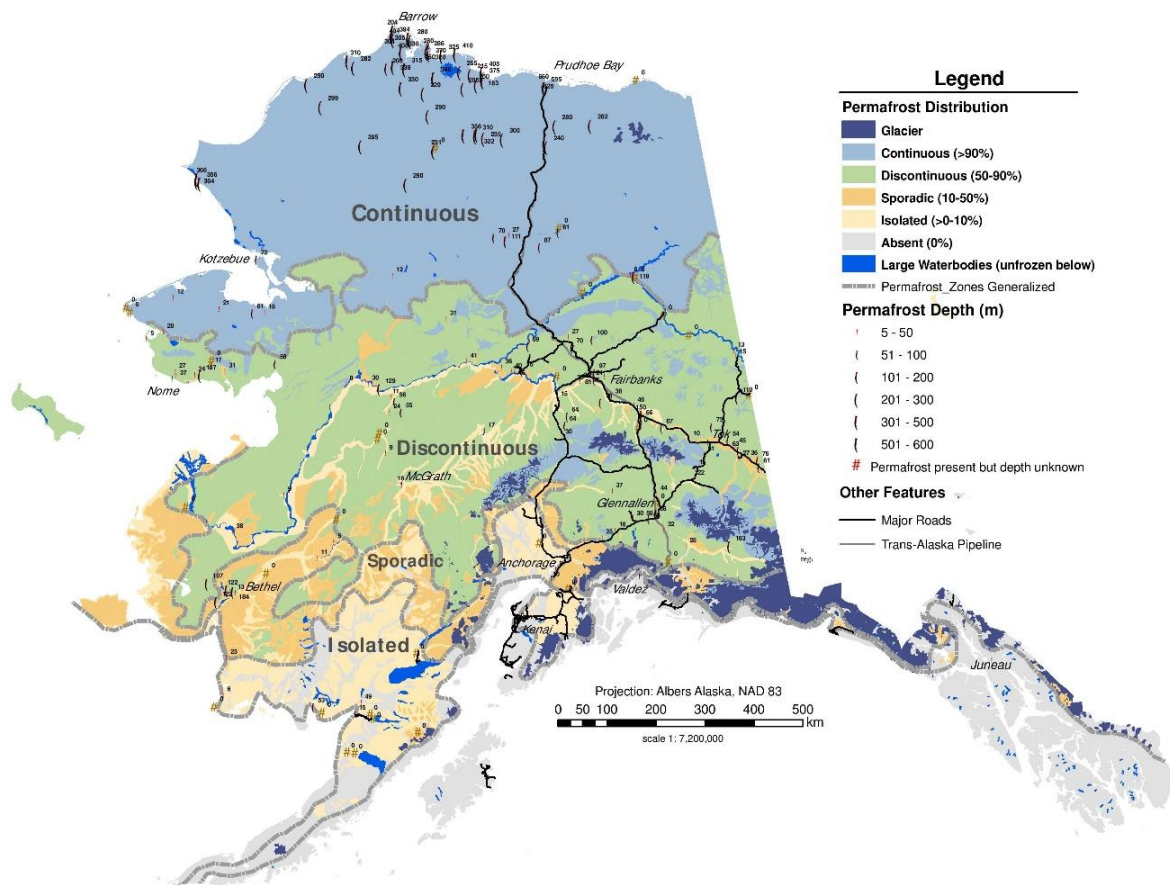
Figure 2: Permafrost Characteristics of Alaska, modified (Jorgenson et al., 2008)

2.2 Influence of periglacial processes on the global carbon cycle

If gases like carbon dioxide and methane enter the atmosphere, the radiant energy from the sun is trapped and redirected to the ground, which heats up. This natural and live supporting effect is disturbed by human activities like burning fossil fuels (Stocker, 2014). Because of global warming, the temperature of permafrost are rising which leads to thawing (Osterkamp, 2005). Permafrost contains around 398 gigatons of thaw-susceptible carbon stored in yedoma, thermokarst lakes and basins (Strauss et al., 2017, Strauss et al., 2013). Thawing permafrost is exposing this organic matter so that microbiological organisms can process it. As a by-product, greenhouse gases such as carbon dioxide and methane are released into the atmosphere and intensify the greenhouse effect (Walter et al., 2006). This leads to more thawing permafrost and finally to further greenhouse gas release. This so called positive feedback loop is one of the main current topics of periglacial research. Thawing permafrost leads to the development of so called thermokarst lakes. Thermokarst is a term related to processes that are influenced by thawing permafrost. The thaw of ground ice leads to the collapse and subsidence of the ground (French, 2013).

The resulting basin is filled with excess water creating ponds and lakes which are described as thermokarst lakes (Fig. 3). Thermokarst lakes act as sinks accumulating high quantities of organic carbon and are considered as a major source of carbon-based atmospheric greenhouse gases, such as carbon dioxide and methane during the Holocene epoch (Walter et al., 2006, Walter et al., 2007, Petrenko et al., 2009, Brosius et al., 2012).Therefore, the understanding of processes revolving the formation and evolution of thermokarst lakes is of great interest for scientist.

The high carbon accumulation result from thermokarst-related shore erosion followed by the deposition of terrestrial organic matter into the lake and the increased aquatic productivity from nutrient supply by thawing permafrost (Walter Anthony et al., 2014). Through the thawing of permafrost and the creation of thermokarst lakes, the prior freeze-locked carbon is reintroduced to the carbon cycle.
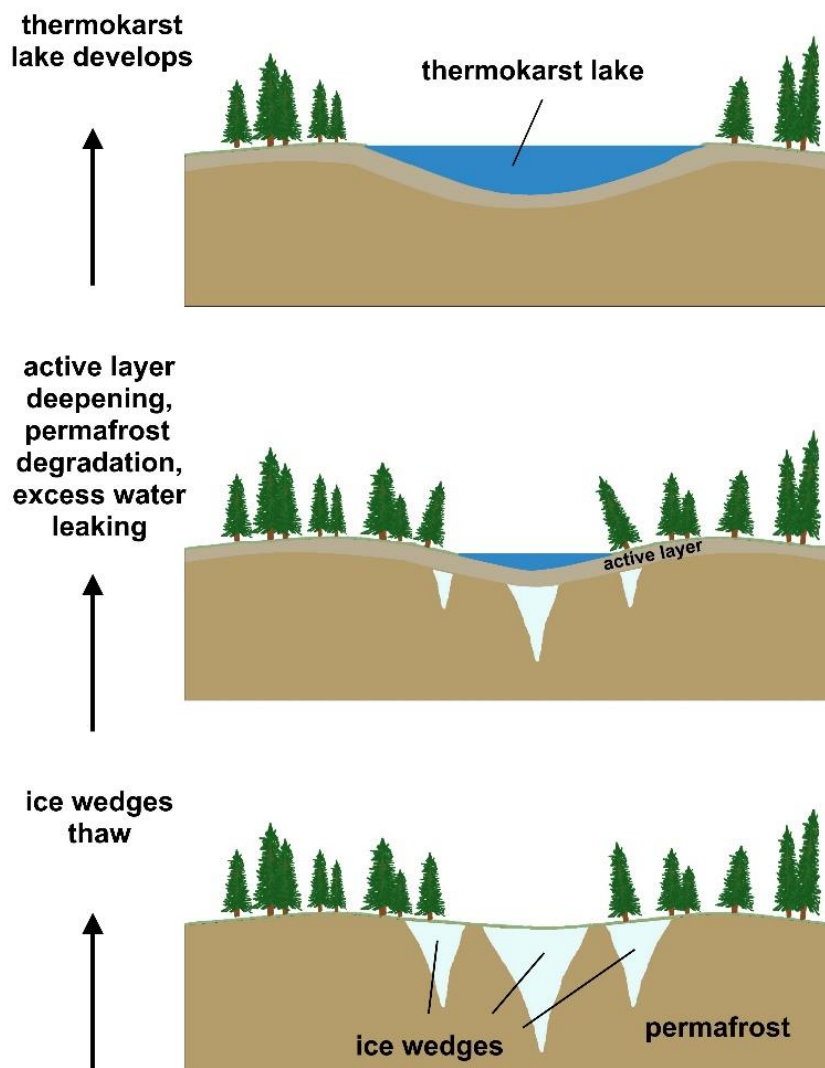
Figure 3: Schematic evolution of a thermokarst lake

2.3 Study Area

The studied lake is situated in the Goldstream Valley in Central Alaska (Fig. 4). Goldstream Lake is located approximately 9 km north from the University of Alaska right next to Ballaine Road at 186 m above sea level.

Goldstream Lake is circa 170 m long and has a surface area of approximately 9350 m^2. The maximum depth is 3.3 m and the mean depth is 1.9 m. Such shallow depths are typical for thermokarst lakes.
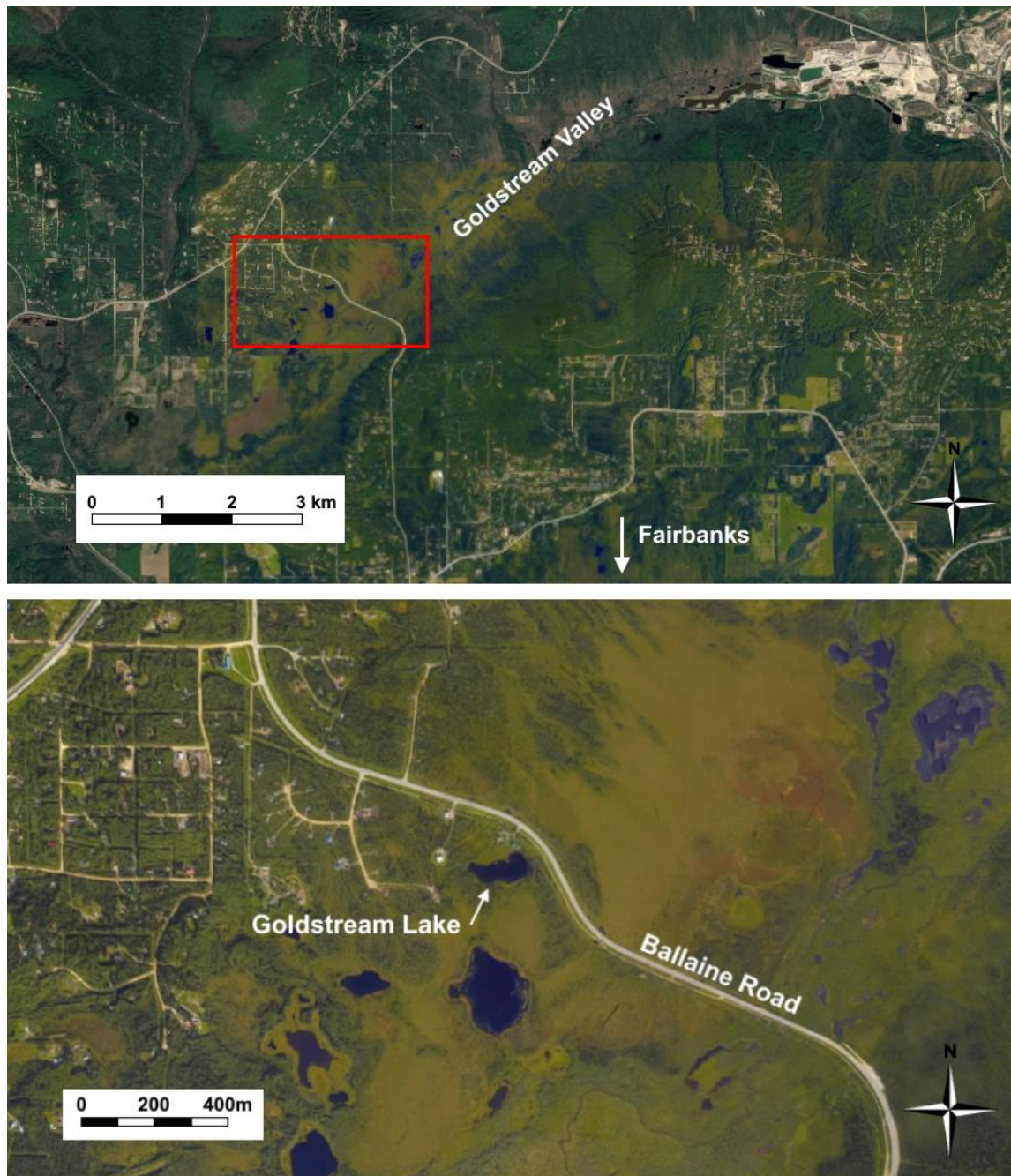
Figure 4: Satellite images of the study area with Goldstream Lake (images from DigitalGlobe, Google 2017)

2.4 Climate

The area around Fairbanks experiences short warm summers and cold long winters classifying as a subpolar climate (Fig. 5). The mean temperature reaches its maximum of 16.9 °C in July and minimum in January with -22.17 °C. The mean Temperature stays below 0 °C between October and March. The most precipitation falls in July with a mean of 54.86 mm. The lowest precipitation falls in March with a mean of 6.35 mm. This data was obtained from the Alaska Climate Research Center weather station which is located on the roof of the Geophysical Institute at the University of Fairbanks (at 64° 51' 22" N, 147° 50' 58"W, 225 m above sea level).
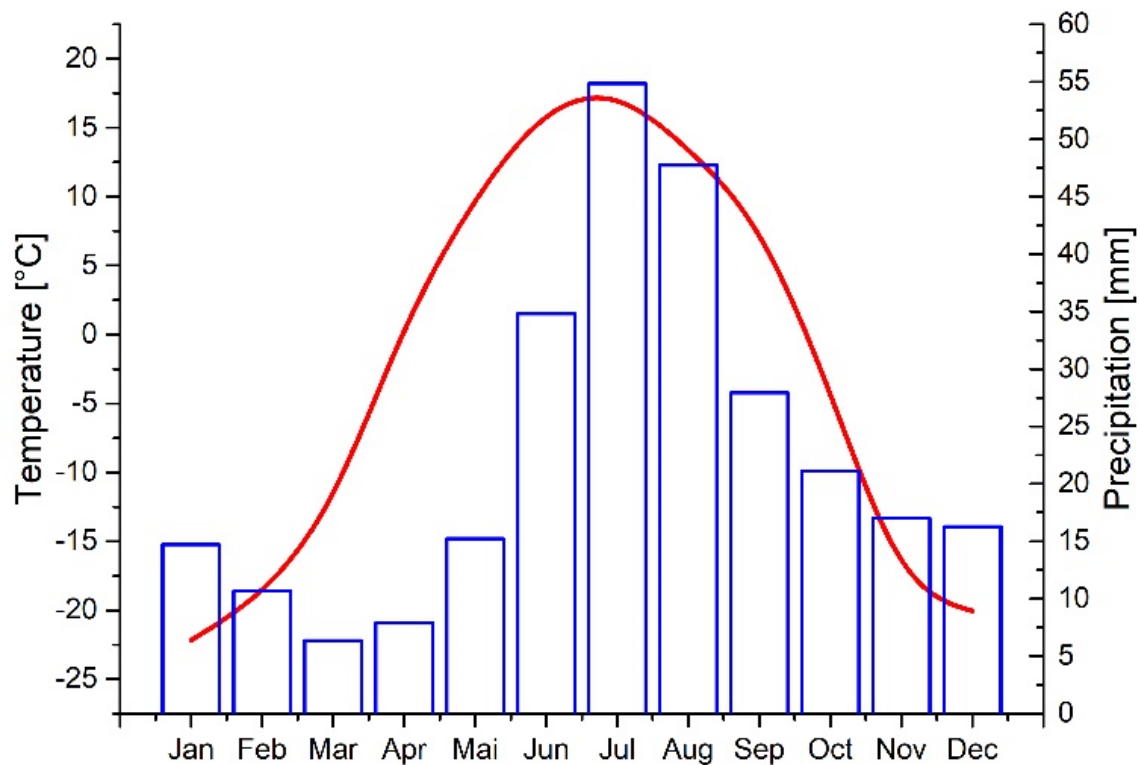
Figure 5: Temperature and Precipitation in Fairbanks, data from the Alaska Climate Research Center at the University of Alaska in Fairbanks (http://akclimate.org/Climate/Fairbanks; 05/10/2017)

2.5 Vegetation and ecosystem

The region around Fairbanks is dominated by coniferous boreal forests (Viereck et al., 1992) and therefore classifies as taiga. South-facing uplands of the region are dominated by *Picea glauca* (white spruce), while poorly drained, north-facing slopes and lowlands are dominated by *Picea mariana* (black spruce) and moss communities. Plants of the species *Typha latifolia* (broadleaf cattail) and *Betula neoalaskana* (paper birch) grow near Goldstream Lake. The amount of phytoplankton from thermokarst lakes in the tundra is rather sparse (Vézina and Vincent, 1997, Elster et al., 1999) in contrast to this lake in the boreal zone which indicates a high bioproductivity (Fig. 6d). Shallow polar ecosystems like thermokarst lakes are typically dominated by cyanobacterial mats and contain a high zooplankton biomass (Rautio and Vincent, 2006).
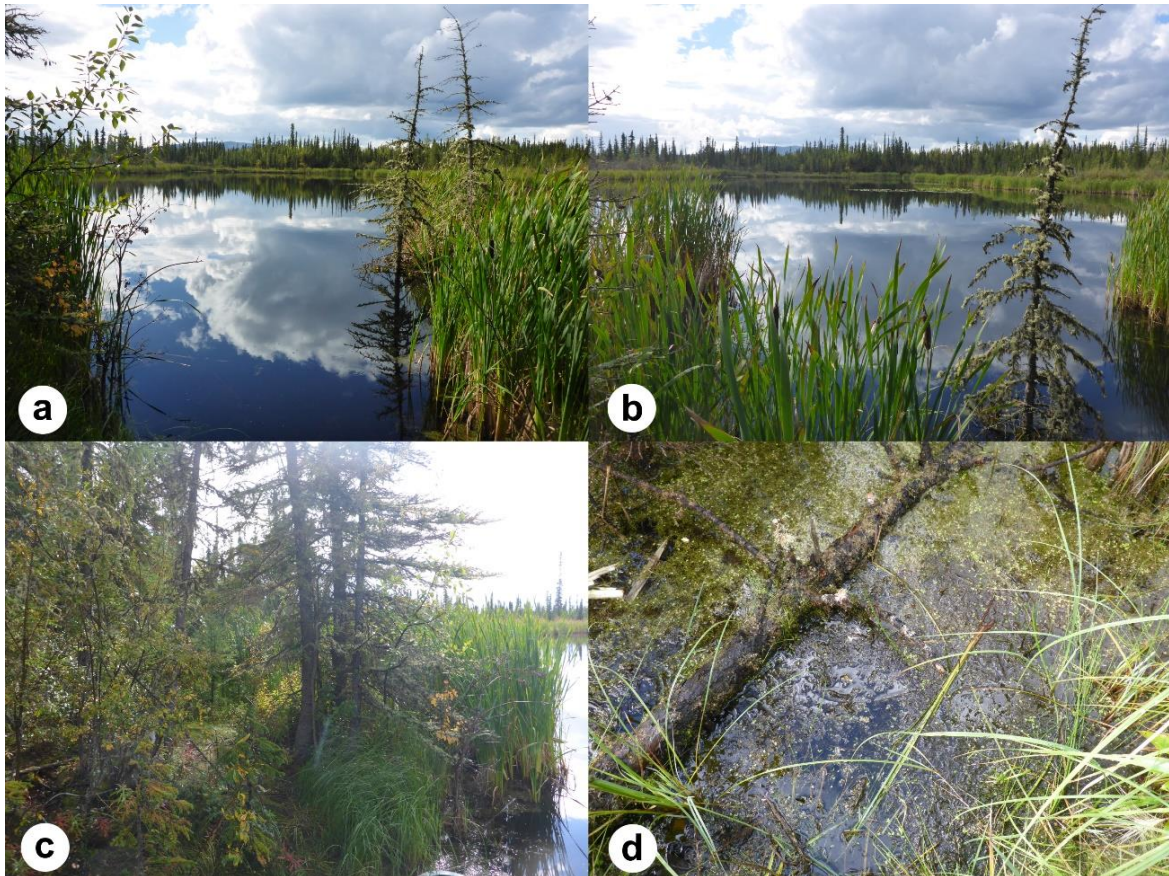
Figure 6: Pictures of the southeastern shore of Goldstream Lake in August 2016; a), b) & c) show broadleaf cattail coniferous and deciduous trees, d) high bioproductivity at the shore

3. Material and Methods

Sediment facies are described visually, and sediment is analyzed for water content, magnetic susceptibility and grain size distribution to characterize physical sediment properties. The total carbon (TC), total nitrogen (TN), total organic carbon (TOC) and stable carbon isotopes (δ^{13}C) is used to identify the origin of organic matter by distinguishing between terrestrial and lacustrine organic matter signals (Fig. 7).
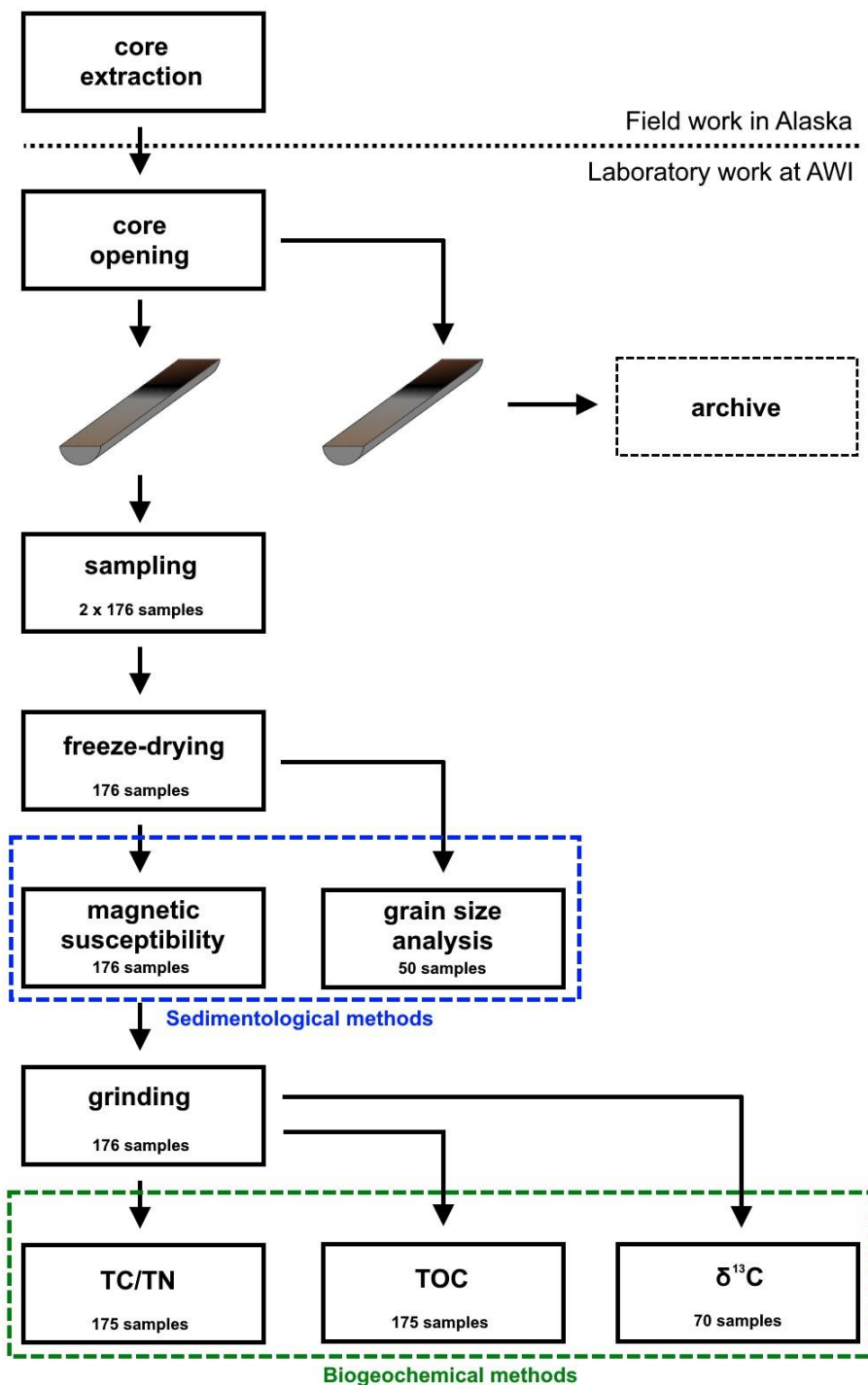
Figure 7: Flowchart of the applied methods

3.1 Field work and Sampling

Four sediment cores with lengths of 137.5 to 382.0 cm were retrieved on March 17th and 18th, 2017 from Goldstream Lake during the PETA-CARB Expedition "Central Alaska 2017" led by Dr. Josefine Lenz (AWI, UAF). The sediment cores were drilled from the lake ice using two different methods, the piston hammer and the vibracore system. The hammer core system (Fig. 8) was used to retrieve shorter cores with potentially less disturbed surface sediments. Here, a PVC tube with a diameter of about 10 cm is pushed into the sediment by pounding a weight continuously on a metal coring head. The vibracore system allows to retrieve long sediment cores of up to 5 m. Here, an aluminum tube is driven into the sediment using a vibration motor. Three cores were drilled with a piston hammer corer (HC) and one core with a vibracorer (VC) from the frozen surface of Goldstream Lake.

Figure 8: Field work at Goldstream Lake; a) opening of the ice at T3; b) vibracore retrieval of T3; c) & d) hammer coring at T1 (Photos by J. Lenz)

One core of 382 cm was obtained from the center of the lake with the vibracorer (T3). Two cores of 144.5 cm and 137.5 cm length were cored at the northeast and southeast shores of the lake (T1, T5). A fourth core was collected between the center and northeastern shore (T2) (table 1 and figure 9).

Table 1: Core ID, coordinates and length of sediment cores from Goldstream Lake.

Core ID	Latitude [°N]	Longitude [°W]	Total core length [cm]
CAK17-GSL-T1-HC2	64.91599	-147.84752	144.5
CAK17-GSL-T2-HC	64.91579	-147.84804	205.0
CAK17-GSL-T3-VC	64.91557	-147.84845	382.0
CAK17-GSL-T5-HC	64.91552	-147.84785	137.5
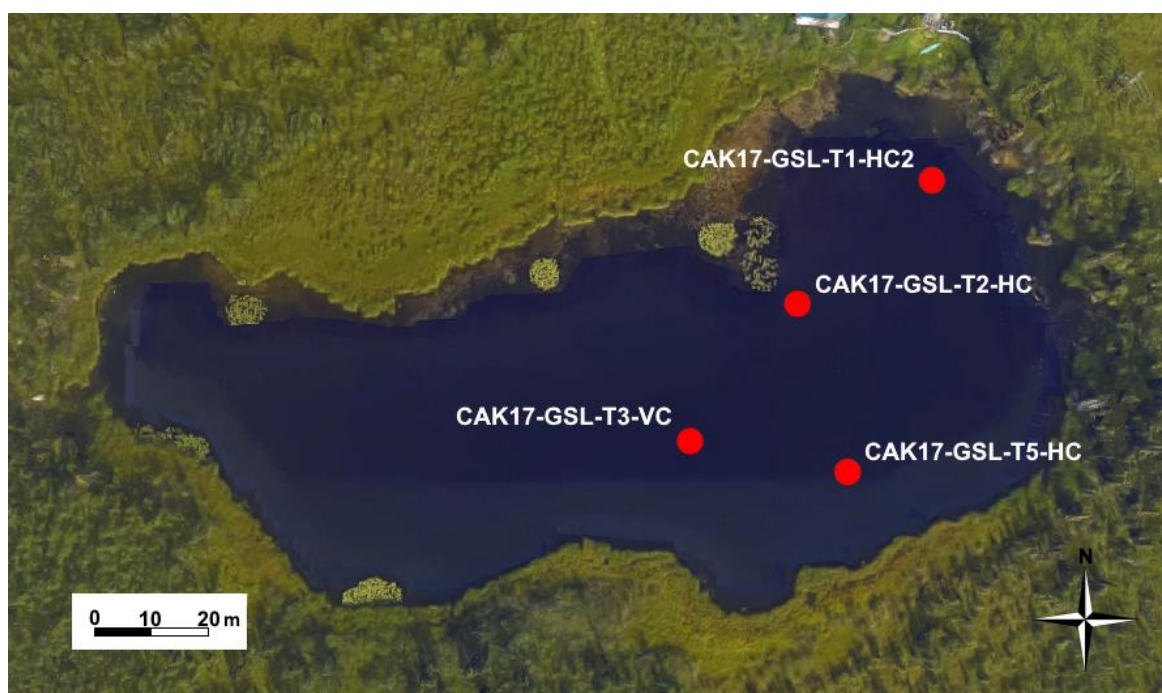
Figure 9: Satellite image of Goldstream Lake with core ID and location (images from DigitalGlobe, Google 2017)

The cores were prevented from freezing and stored cool during their transportation to the laboratories of AWI Potsdam.

The cores were cut in half using a *Fein MultiMaster* and two 6 cm^3 samples were taken nearly every 5 cm. A total of 2 x 176 samples was taken. The samples were dried, and the water content was calculated through the weight difference between the wet sample and the dried sample. The magnetic susceptibility was measured before one half of the samples was grinded and homogenized. These grinded samples were used for the element analysis and stable carbon isotope analysis. The other half of the samples was used for the grain size analysis.

3.2 Sedimentological methods

3.2.1 Magnetic Susceptibility (MS)

The magnetic susceptibility (MS) describes the ability of a material to be magnetized in an external field (Bartington-Instruments, 2017). It can be used to differentiate between different facies and mineralogical components, that are not visible with the naked eye. It was measured using the *Bartington instruments magnetic susceptibility meter MS2* and a *sensor type MS2B Dual Frequency*. The instrument is magnetizing a sample by generating a magnetic field. The following change of inductance in the inductor can be detected by the instrument. The *sensor type* MS2B is able to measure the magnetic susceptibility of a sample with a low and a high frequency (Bartington-Instruments, 2017). A total of 176 samples were measured using the low frequency setting.

3.2.2 Grain size analysis

The organic matter was removed from every sample in order to analyze the grain size of the minerogenic compounds. A selection of 50 samples were put in separate beaker and mixed with 100 ml of a 3 % hydrogen peroxide solution and four drops of ammonia. The beakers were then placed and heated on a shaker for 2 weeks. The pH of the samples was measured regularly and maintained at a pH of 6.5 to 8 to ensure a constant maximum reaction between the H_2O_2 and the organic matter in the sample. In addition, 10 ml of a 30 % H_2O_2 solution were added to the beakers every second day to maintain a constant reaction. After the removal of organic matter, the H_2O_2 was washed out with desalinated water. Tetrasodium pyrophosphate 10-hydrate was added to the sample, to prevent the particles from agglutinating. The grain size was measured using the *Malvern Mastersizer 3000*, a laser diffraction particle size analyzer. The particle size analyzer uses a laser beam, passing through a dispersed particulate sample. The laser beam hits a particle and is then scattered. The angular variation of the scattered light is then measured. The intensity of the scattered light is detected. Smaller particles scatter the laser beam at larger angles then larger particles. The particle size is calculated with the scattering pattern using the Mie theory of light scattering (Handbook Malvern Mastersizer 3000).

3.3 Biogeochemical methods

3.3.1 Element analysis: TC, TN, TOC

The total carbon (TC) and total nitrogen (TN) contents were measured quantitatively using a *elementar vario el III* thermal conductivity detector. A total of 176 grinded samples were weighed into tin capsules. Barium oxide was added to 5 mg of a sample to ensure that the sample would burn completely in the *VARIO EL III* furnace. Two tin capsules were weighed for every sample. The tin capsules were then released into the detector using a sample disposer. The sample components are transported with the carrier gas helium into the measuring channel of the detector. A second measuring channel is used as a reference channel and is only filled with pure carrier gas. Both channels have a build in electrically heated resistance wire. As the sample components pass these resistance wires, the heat dissipation is changed which causes a change in temperature and thus a change in electrical resistance within the wires. Both resistances are compared and converted through a Wheatstone bridge into a current and voltage signal. The signal is directly proportional to the TC and TN concentration in the sample. The standard deviation is better than 1 %.

The total organic carbon contents of the sample were measured using a *elementar vario MAX C* gas-chromatograph. A total of 176 grinded samples were weighed into small metal crucibles. The quantity of the sample weight depended on the measured TC of the sample. The higher the TC in the sample, the less sample material was weighed into the crucible. The weighed amount was limited between 5 and 100 mg. The TOC is driven out under inert gas and oxidized on CuO. The sample is then burnt in the crucible with the addition of oxygen and the produced CO_2 is analyzed via IR-detection.

3.3.2 Stable carbon isotopes ($\delta^{13}C$)

The samples were decarbonated using 1.3 molar hydrochloric acid and placed on a heater to accelerate the reaction. After the decarbonation process, the samples were dried and homogenized. The stable carbon isotopes were measured using a *ThermoFisher Delta-V-Advantage* gas mass spectrometer equipped with a *FLASH elementar analyser EA 2000* and a *CONFLO IV* gas mixing system for the online determination of the carbon isotopic composition. An autosampler system *MA200R* allowed a measurement of 62 samples consisting of 50 sediment samples and 12 standards. An aliquot of a sample is weighed into a tin capsule. According to the TOC content, the quantity of the sample reach from 1 mg to 80 mg. The sample is combusted at 1020°C under an O_2 atmosphere. The resulting CO_2 gas is separated from other gases in a reduction tube and the element analyzer. The CO_2 gas is then transferred to the mass spectrometer using the *CONFLO IV* gas mixing system and a capillary. Helium serves as a carrier gas. The carbon isotope ratio is determined relative to a laboratory standard of known isotopic composition. A quantity of 11 samples were measured for T1. 17 samples were measured for T2. For the longest core T3, 31 samples were measured. The shortest core T5 was measured with 10 samples. The standard deviation is generally better than ±0.15 ‰

4. Results

Different facies can be described through the visual description of the four cores. The lake-central core T3 consists of three facies. Facies 1 describes a fine-grained, dark olive-grey, fine-layered minerogenic sediment. Facies 2 shows a black to brown and organic layer with poorly decomposed sedges, mosses and roots. Facies 3 consists of a fine-grained, grey, non-layered, marbled sediment. Core T2 shows the same number of facies, however, with fewer samples of facies 3. Core T1 only represents facies 1 and 2, while T5 only represents facies 1.

4.1 CAK17-GSL-T1-HC2

Core CAK17-GSL-T1-HC2 is dominated by minerogenic sediment with intermittent well to poorly decomposed organic matter. Near the sediment surface, a well decomposed, black, organic layer (Munsell Soil Color Chart, ID 5Y 2.5/1 (Munsell, 2013)), is followed by very dark grey, minerogenic-organic sediment (5Y 3/1) with coarse organic remains (rootlets) in depth of 16-39 cm. A smooth transition follows to a very dark grey unit (5Y 3/1) with gradually less organics from 39 to 73 cm and minerogenic sediment (5Y 3/1) with some organic remains from 73 to 142.5 cm. A black, poorly decomposed organic matter is located at 144.5 cm. Larger organic remains are: an 8.5 cm piece of wood at 0 cm depth and a piece of wood of 5 and 2 cm length at 30-33 cm and 77.5-78.5 cm. Well preserved *Betula* bark of 9 cm was found at 114-123 cm that was potentially moved down while opening the core.

The water content describes a decrease from 62.7 wt% at the top of the core to a water content of approximately 21 wt%. A small peak of 36.7 wt% can be seen at a depth of 95 cm. The water content increases again at 140 cm from 25.9 wt% to 47.6 wt% at 143 cm (Fig. 11).

The MS ranges from a minimum of 32.40 to a maximum of 140.90. It shows a major increase at 0 to 35 cm and 70 to 80 cm. At 80 cm the MS decreases with slight variations to a depth of 143.5 cm.

Results from grain size analyses range from 0.357 to 1110 µm (coarse clay to coarse sand) (Fig. 10). A larger spread in grain sizes can be seen in the sample close to the surface (at 8 cm) with a higher content of fine silt and clay. The samples from 36 to 144 cm describe a smaller spread in grain sizes and are dominated by coarse silt and fine sand.
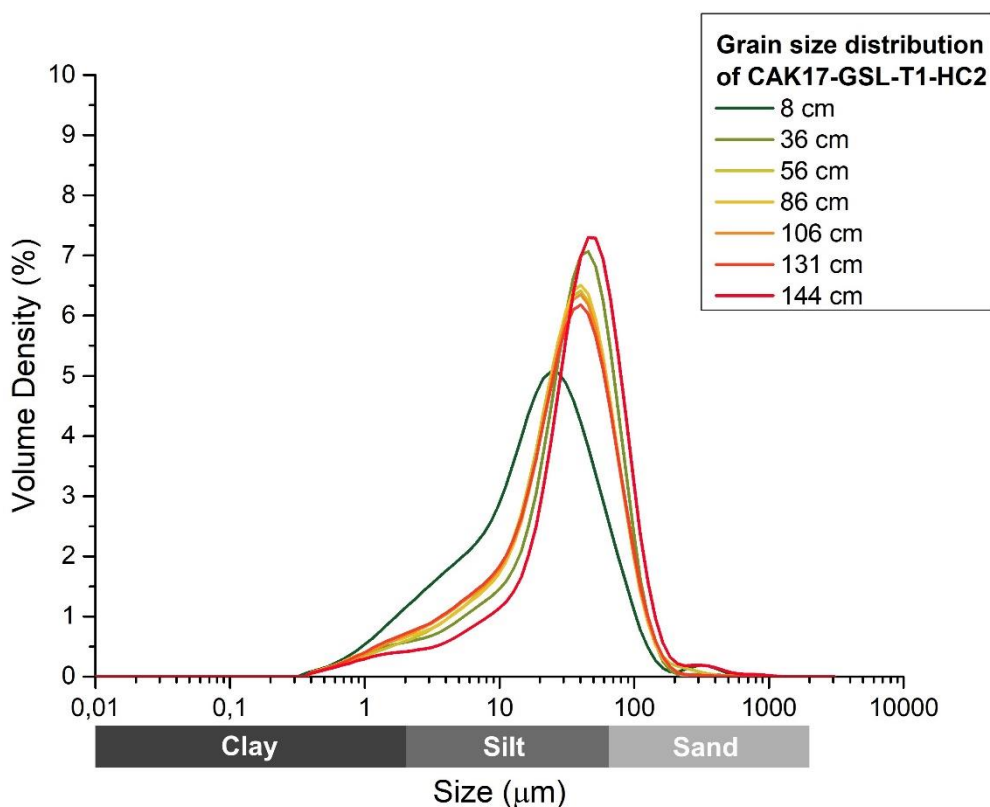
Figure 10: Grain size distribution for CAK17-GSL-T1-HC2

The TN content shows a maximum of 0.345 wt% at the top and is 0.197 wt% on average with the exception of some samples that show a TN below detection limit of 0.1 wt% and are located mainly between 116 - 152 cm and 178 – 198 cm.

The TC is 1.71 wt% on average and shows a maximum at 7 cm with 4.879 wt% and another maximum at 143 cm with 4.17 wt%. The lowest TC can be found at 80 cm with 0.80 wt%.

The TOC follows the same pattern as it is the organic content of the TC with maxima at the top and bottom of the core. At 2 cm the TOC reaches 3.934 wt% and 3.670 wt% at 143 cm. The TOC is 1.55 wt% on average with exception of one sample at 80 cm below the detection limit of 0.1 wt%.

The stable carbon isotopes indicate an average of -27.20 ‰ with a minimum of -29.69 ‰ at the top. The $\delta^{13}C$ increases from this minimum to -24.68 ‰ where it reaches its maximum. From 100 cm the $\delta^{13}C$ decreases again and reaches -29.35 ‰ at 143 cm.
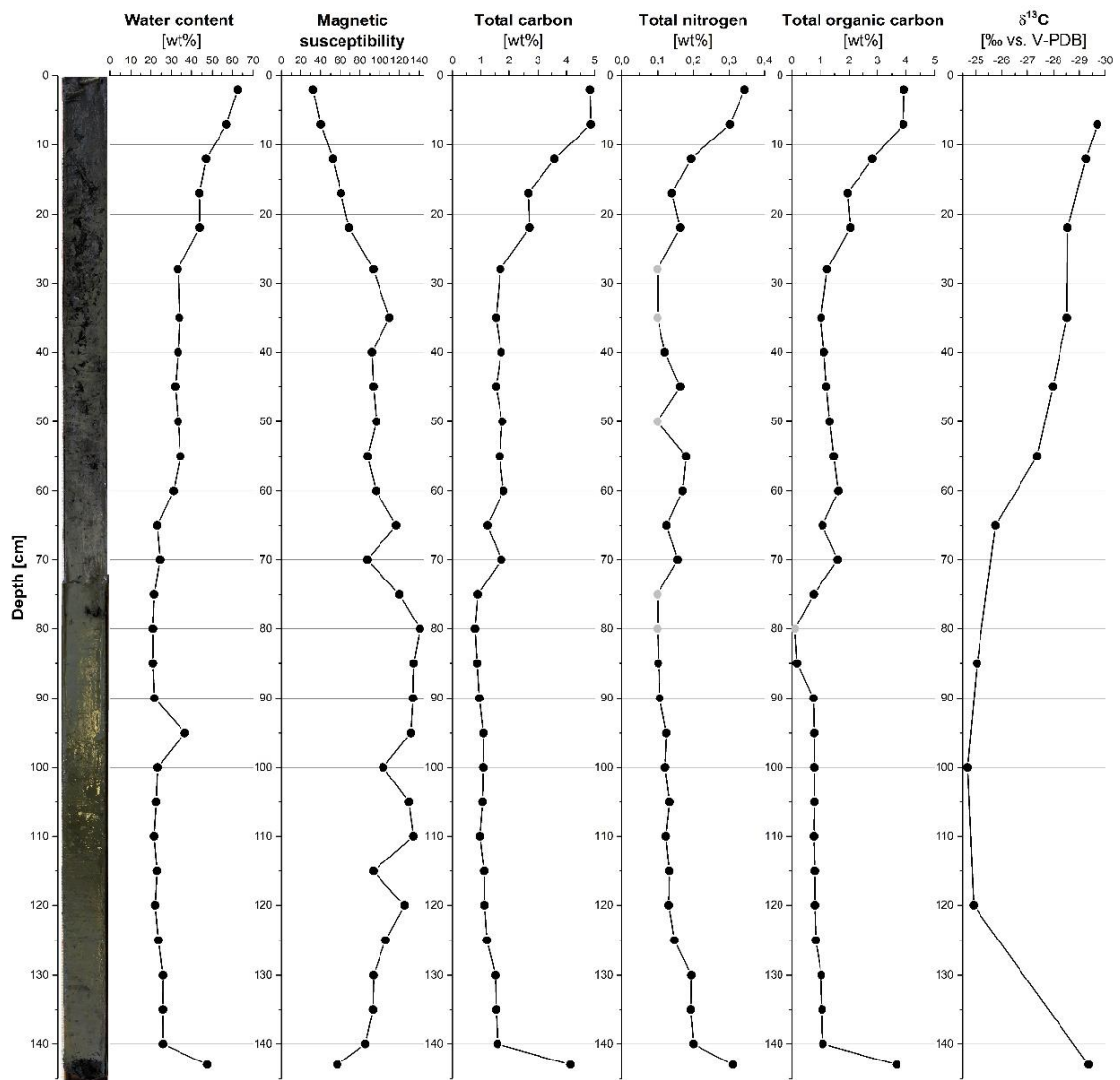
Figure 11: Core picture, water content, MS, TC, TN, TOC, δ¹³C of near-shore sediment core CAK17-GSL-T1-HC2

4.2 CAK17-GSL-T2-HC

Sediment core CAK17-GSL-T2-HC is dominated by minerogenic sediment with no living aquatic vegetation on top and occasionally occurring fine layers of decomposed organic matter. There is homogenous minerogenic, dark grey sediment (5Y 4/1) with almost no visible organic remains for the first 24 cm. Between 24 and 50 cm are olive grey, minerogenic sediments (5Y 4/2) with varying grain sizes and no organic remains followed by a black, very fine decomposed organic layer of 0.5 cm and a 2.5 cm thick brown decomposed organic layer (10YR 3/1) with minerogenic compounds. From 53 to 66 cm there is very dark grey, minerogenic sediment (5Y 3/1) with no visible organic remains, followed by an organic layer (66-78cm) with finely decomposed organics on top (rootlets) to poorly decomposed organic remains at the bottom. A Caddisfly (*Trichoptera*) case was found at 75 cm. A homogenous black minerogenic sediment (5Y 2.5/2) with very few organic remains reaches from 78 to 156 cm followed by a 5 cm thick, poorly decomposed peat layer (155-160 cm) with 7cm long and wooden remains with well-preserved bark. The peat layer is followed by a very dark grey layer (5Y 3/1) of minerogenic sediment with organic remains at 160-164 cm and an organic lense at 163-164 cm. The core ends with minerogenic sediment (5Y 2.5/1) with darker organic layers and lenses (10YR 3/1) at 171-177 cm,191-193 cm and 203-205 cm.

The water content stays at an average of 20-25 wt% throughout the core with individual peaks at 51 cm with 35.9 wt%, at 71 cm with 58.5 wt%, at 159 cm with 52.2 wt% and at 164 cm with 44.5 wt% (Fig. 13).

The MS reaches 122.30 at 2 cm and decreases with little changes from 125.75 at 30 cm to 16.43 at 75 cm where it reaches its minimum. A major increase follows with 151.50 at 91 cm. Between 101 cm and 173 cm the MS ranges from 36.70 and 126.53. At 188 cm the MS reaches its maximum with 170.87. The MS is 98.33 on average.

The grain sizes range from 0.357 to 586 µm which classifies as medium clay to medium sand. From 8 to 57 cm (Fig. 12, green lines) the samples are rich in coarse silt with exception of the sample at 31 cm which has a wider stretch with a higher content of fine silt and coarse clay. The samples from 68 to 131 cm show a high content of coarse silt to fine sand and a relatively small spread on other grain sizes. The bottom samples, ranging from 153 to 204 cm indicate a larger spread of different grain sizes with higher contents of coarse clay, fine silt and medium silt compared to the samples that are closer to the sediment surface.
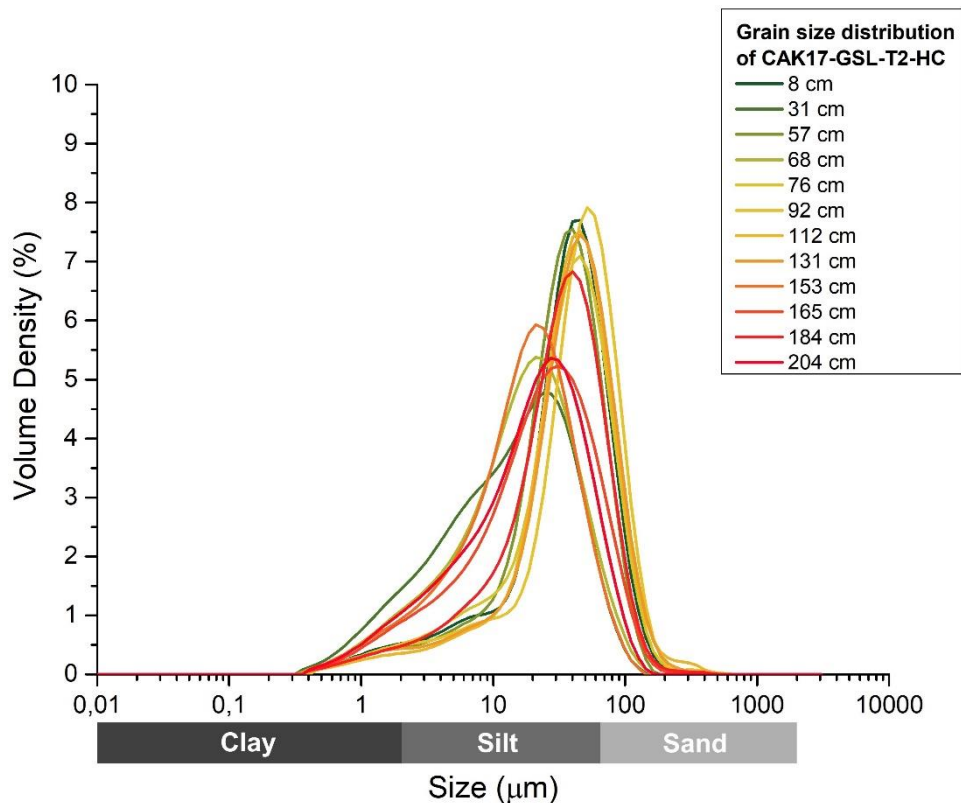
Figure 12: Grain size distribution for CAK17-GSL-T2-HC

In 19 of the 40 samples the TN show a value below the detection of 0.1 wt%. The first samples ranging from 2 to 51 cm have a TN between 0.11 wt% and 0.21 wt%. At 71 cm the TN reaches a global maximum of 0.58 wt% and smaller peaks at 159 cm with 0.35 wt% and at 164 cm with 0.37 wt%.

The TC stays at approximately 1 wt% with some major peaks. The first peak increases from 0.73 wt% at 61 cm to 5.81 wt% at 71 cm and decreases again to 0.81 wt% at 81 cm. The next major peaks occur at 159 cm with 7.82 wt% where the TC reaches its maximum and at 164 cm with 7.03 wt%.

The TOC follows the same pattern and stays at around 0.8 wt% throughout the core. Major peaks appear at 71 cm with 5.57 wt %, at 159 cm with 7.82 wt% where the TOC reaches its maximum and at 164 cm with 6.82 wt%.

The stable carbon isotopes show an average of -26.27 ‰ with a maximum of -24.91 ‰ at 7 cm. The δ^{13}C decreases slightly to -25.21 ‰ at 46 cm and shows a major decrease and global minimum at 67 cm with -28.38 ‰. An increase occurs and the δ^{13}C stays between 86 and 136 cm at -25.78 ‰ and -25.47‰. Local minima appear at 159 cm with -28.25 ‰ and at 173 cm with -27.05 ‰.
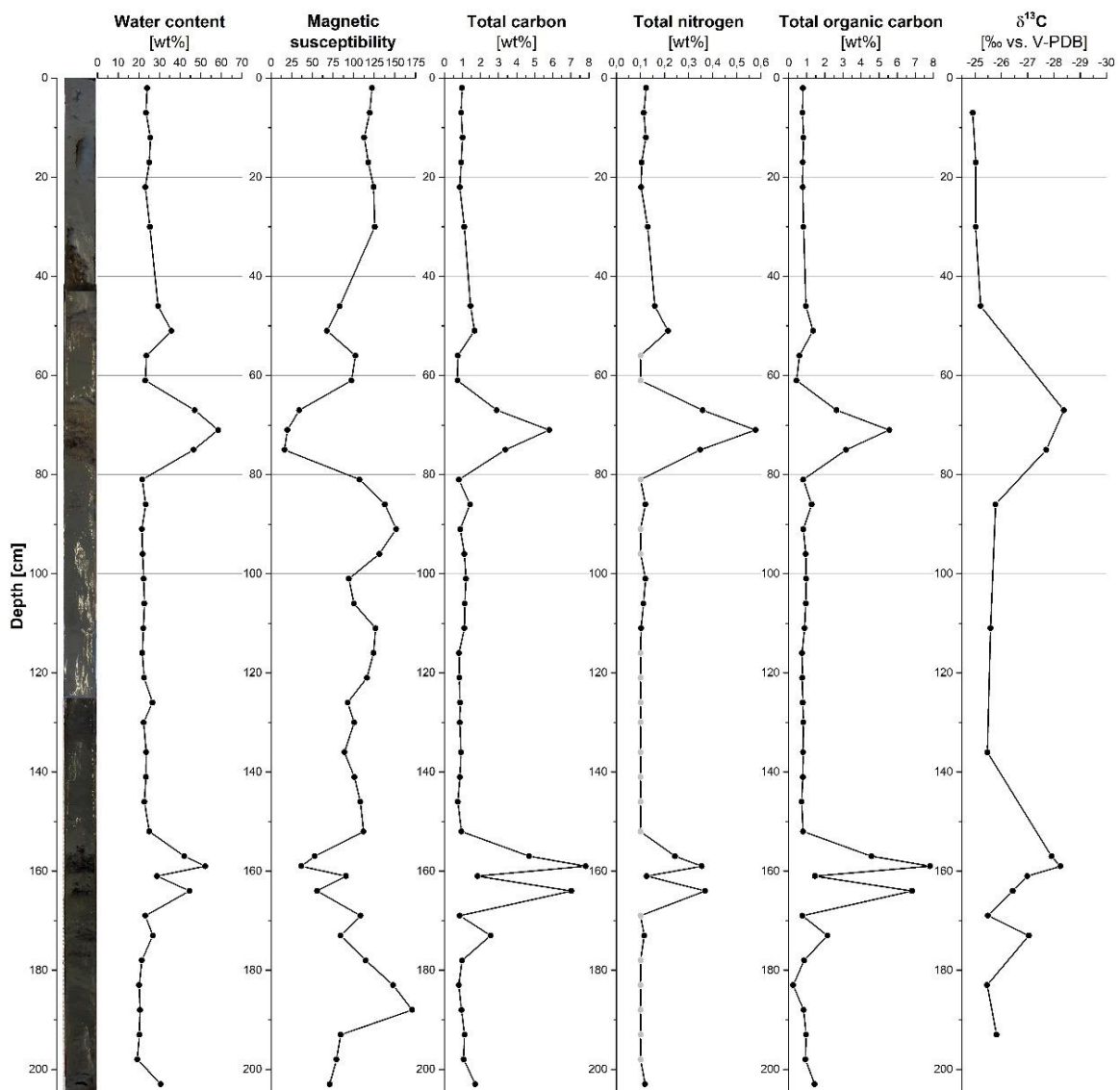
Figure 13: Core picture, water content, MS, TC, TN, TOC, δ^{13}C of sediment core CAK17-GSL-T2-HC

4.3 CAK17-GSL-T3-VC

Sediment core CAK17-GSL-T3-VC is a dark grey, minerogenic sediment (5Y 4/1) from 0 to 144 cm. It is homogenous for most parts but clearly, lighter and finer layered at 2-10 cm (0.5-1 mm thick layers), 25-32 cm (gradual from fine silt to clay) and at 100-109 cm (3-5 mm thick layers). Organics can be found in dark decomposed layers (2-4 cm and 56-58 cm) and in form of larger remains of up to 7 mm in 70 cm depth. From 114 to 140 cm there is fine, minerogenic and layered sediment (5Y 4/1) with distinct dark 2-4 mm thick layers of well decomposed organics at 114-115, 120-122, 129-130 and 136-139 cm. A poorly decomposed peat layer (140-149 cm) with sedges, mosses and roots is followed by a diagonal transition to a black, well decomposed organic layer (10YR 2/1) with minerogenic compounds at 149-155 cm. Minerogenic sediment (5Y 2.5/1) occurs between 155 and 173 cm with darker layers that are not clearly distinct but seem to be marbled. An otherwise largely homogenous minerogenic unit from 173 to 310 cm seems to have a non-layered marbled sediment (5Y 4/1) from 280 to 310 cm as well. The part from 310 to 382 cm is similar to the overlying unit with marbled minerogenic-organic sediment (5Y 3/1) but with a higher amount of organic remains.

A water content of 36.6 wt% occurs at 1 cm and stays at an average of 27.2 wt% from 6 to 112 cm. At 112 cm the water content increases to 54.2 wt% at 121 cm. A major peak occurs at 147 cm with 69.2 wt%. At 186 cm the water content reaches a minimum of 15.9 wt% from where it increases slowly to 33.2 wt% at 365 cm (Fig. 15).

The MS increases heterogeneous from 56.7 at 1 cm to 117.2 at 80 cm where it reaches its local maximum. The MS reaches a local minimum at 121 cm with 31.15 where it increases again to 100.27 at 126 cm. The global minimum occurs at 147 with 6.85. The MS reaches its global maximum with 131.10 at 191 cm. From 211.5 to 381.5 cm the MS follows an average of approximately 88 wt% with a local minimum at 335 cm with 55.75 and two smaller peaks at 350 cm with 105.05 and at 374 cm with 110.45.

The particle analysis for T3 (Fig. 14) shows a relatively heterogenous distribution of grain sizes for the first 151 cm from the surface. The grain sizes range from 0.314 to 666 µm which classifies as medium clay to coarse sand. Whereas samples at 6, 21, 85, 107, 115 and 137 cm show a higher content of medium silt, samples at 41, 62, 126 and 151 cm show higher contents of coarse silt. The samples between 156 cm and 305 cm show a relatively homogenous distribution of grain sizes with a smaller spread ranging from medium clay with 0.357 µm to medium sand with 454 µm. All samples between 156 cm and 305 cm show a

maximum peak at coarse silt with approximately 40 µm. Samples ranging from 315 cm to the bottom of the core show a similar homogenous distribution of grain sizes but with higher contents of finer particles. The grain sizes range from medium clay with 0.357 µm to medium sand with 454 µm. The samples between 315 cm and 381.5 cm show a maximum peak at coarse silt with approximately 31 µm.
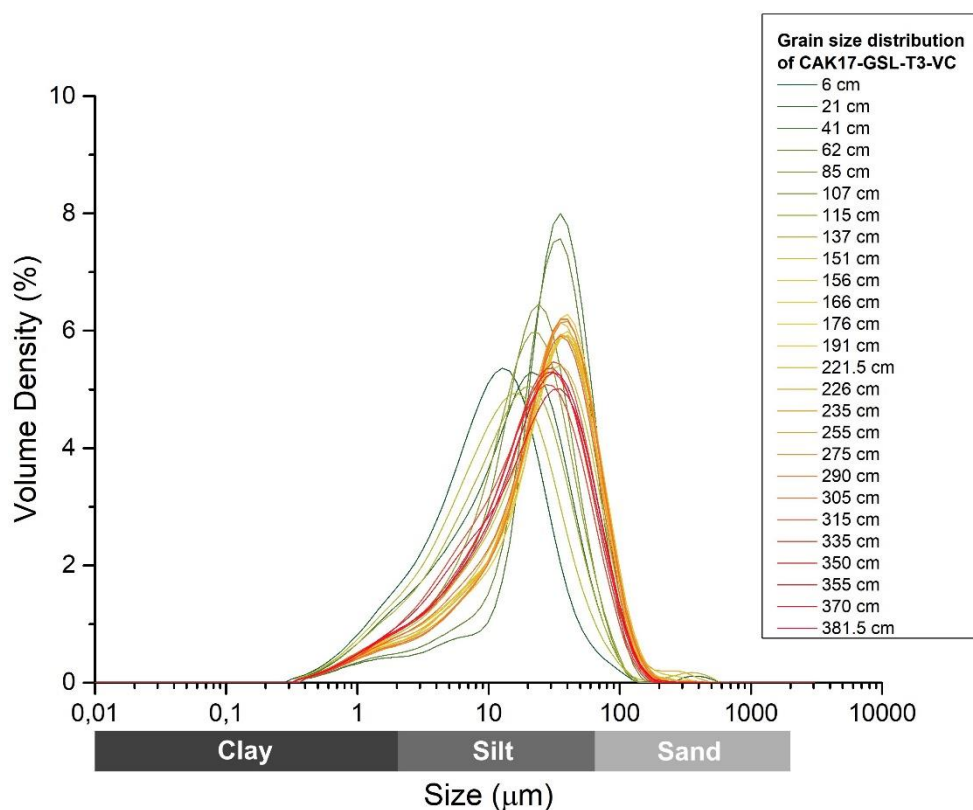
Figure 14: Grain size distribution for CAK17-GSL-T3-VC

The TN for T3 shows a value below the detection limit of 0.1 wt% for 41 of the 78 measured samples. Some smaller TN values appear at the sediment surface ranging from 0.12 wt% to 0.16 wt% and at the bottom ranging 0.11 wt% to 0.29 wt %. A small peak occurs at 121 cm with a TN of 0.59. A maximum is reached at 147 cm with 1.30 wt%.

The TC stays predominantly at approximately 1.5 wt%. The exceptions are two major peaks at 121 cm with 7.03 wt% and at 141 - 147 cm with 17.82 – 28.35 wt%. At the bottom of the core the TC rises from 1.29 wt% at 300 cm to 3.42 wt% at 340 cm and decreases from 3.00 wt% at 365 cm to 1.88 wt% at 381.5 cm.
The first sample at 1 cm has a TOC of 1.475 wt% which decreases slightly to an average of approximately 0.8 wt%. This average holds up to 112 cm were the TOC peaks with 7.03 wt% at 121 cm. A following peak occurs at 141 – 147 cm with 17.51 – 29.03 wt% and

forms a global maximum. Between 221 cm and 381.5 cm an average of approximately 1.2 wt% with little variations is met. Eight Samples were measured with a TOC below the detection limit of 0.1 wt%.

The stable carbon isotopes show an average of -25.47 ‰ between 3 cm and 112 cm. A major decrease follows at 121 cm with -31.06 ‰ which slowly increases to -25.93 ‰ at 171 cm. From 211 cm to the bottom of the core the δ^{13}C shows only little variation with an average of -24.72 ‰.
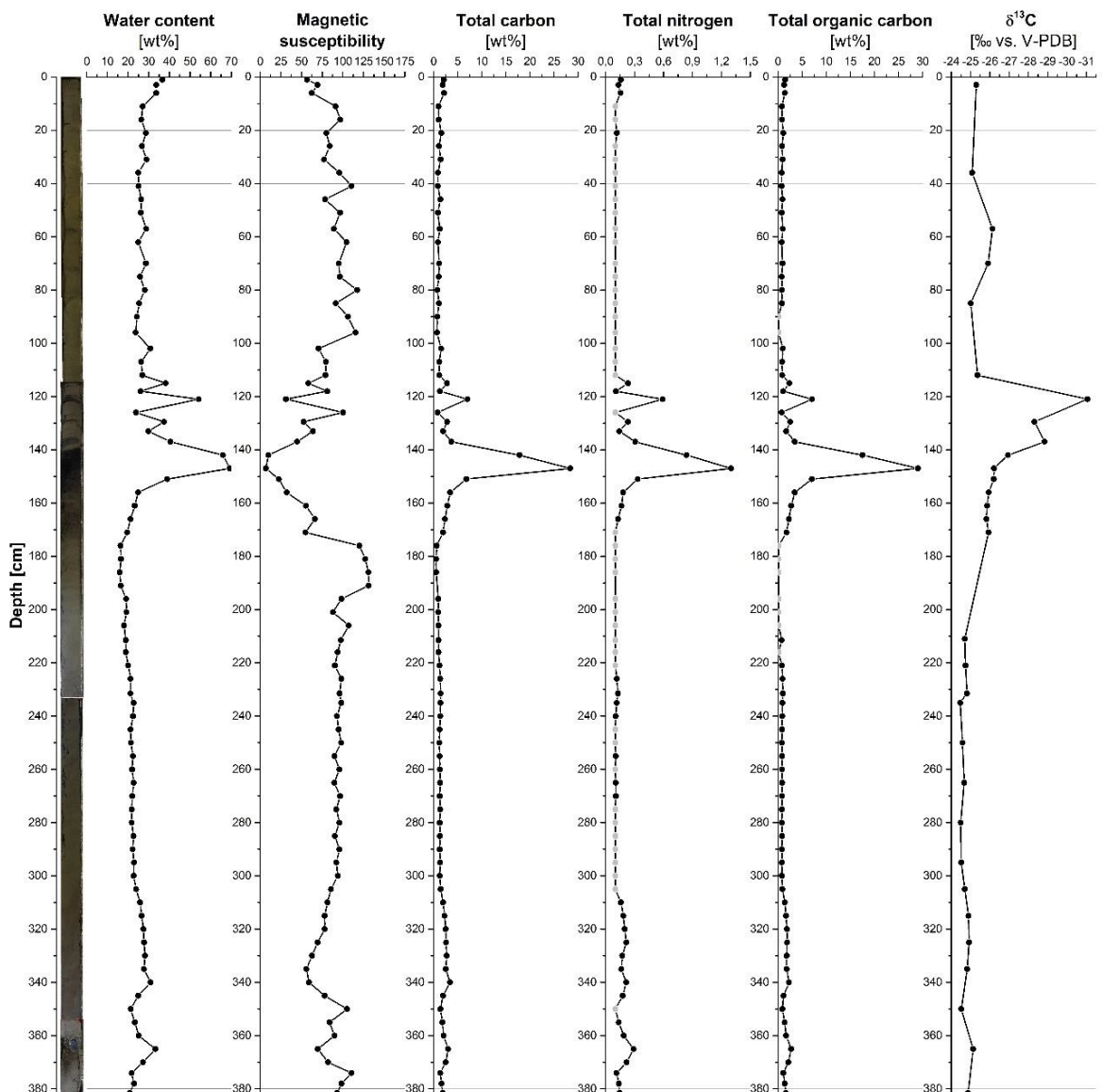
Figure 15: Core picture, water content, MS, TC, TN, TOC, δ13C of CAK17-GSL-T3-VC

4.4 CAK17-GSL-T5-HC

Core CAK17-GSL-T5-HC is dominated by homogenous minerogenic sediments (5Y 3/1). There are few darker, possible organic-rich layers visible at 42, 83, 86, 102, 120 and 127-134 cm. An inclusion (5Y 2.5/2) with very small rootlets is found at 53-62 cm. A 5 mm piece of charcoal is found at 129 cm.

The water content for T5 indicates an average of 25.5 wt%. It ranges from 30.4 wt% at 2 cm to 21.7 wt% at 135 cm following a nearly linear progression with one exception at 68 cm where the water content reaches 39.7 wt% (Fig. 17).

The MS indicates an average of 96.00 starting at 2 cm with 71.80 end ending at 135 cm with 115.95. The progression indicates only small variations with no clear peaks, only smaller maxima at 63 cm with 123.20 and at 75 cm with 121.17.

The grain sizes for T5 (Fig. 16) range from 0.357 to 2,710 µm which classifies the grains from medium clay to very fine gravel. The samples at 12 cm and 49 cm show a wider distribution of grain sizes peaking at coarse silt with approximately 26 µm. A very small percentage of 0.028 vol% of coarse particles appear in sample 49 between 666 µm and 2,710 µm. The sample at 81 cm and 126 cm show a smaller distribution and a higher percentage of coarse silt with an average of 42.85 µm.
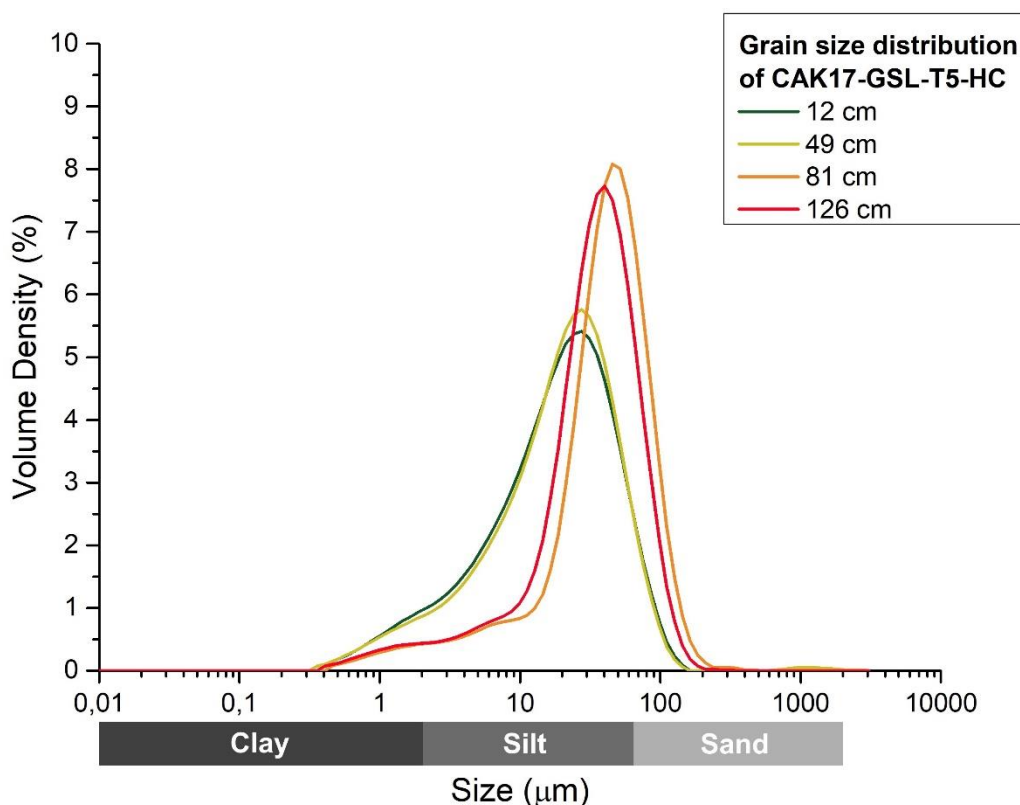
Figure 16: Grain size distribution for CAK17-GSL-T5-VC

The TN for T5 shows only 3 values above the detection limit. The TN shows 0.132 wt% at 2 and 7 cm and 0.102 wt% at 42 cm.

The TC ranges from 1.50 wt% at 2 cm to 1.02 wt% at 135 cm and indicates an average of 1.09 wt%. The maximum is reached at 42 cm with 1.58 wt% and the minimum occurs at 75 cm with 0.60 wt%.

The TOC ranges from 0.93 wt% at 2 cm to 0.79 wt% at 135 cm and shows an average of 0,778 wt% with exception of one sample at 68 cm with a TOC below the detection limit. One local minimum appears at 110 cm with 0.146 wt%.

The stable carbon isotopes show very little variation, ranging from -25.05 ‰ at 2 cm to -25.34 ‰ at 135 cm with an average $\delta^{13}C$ of -25.21 ‰.
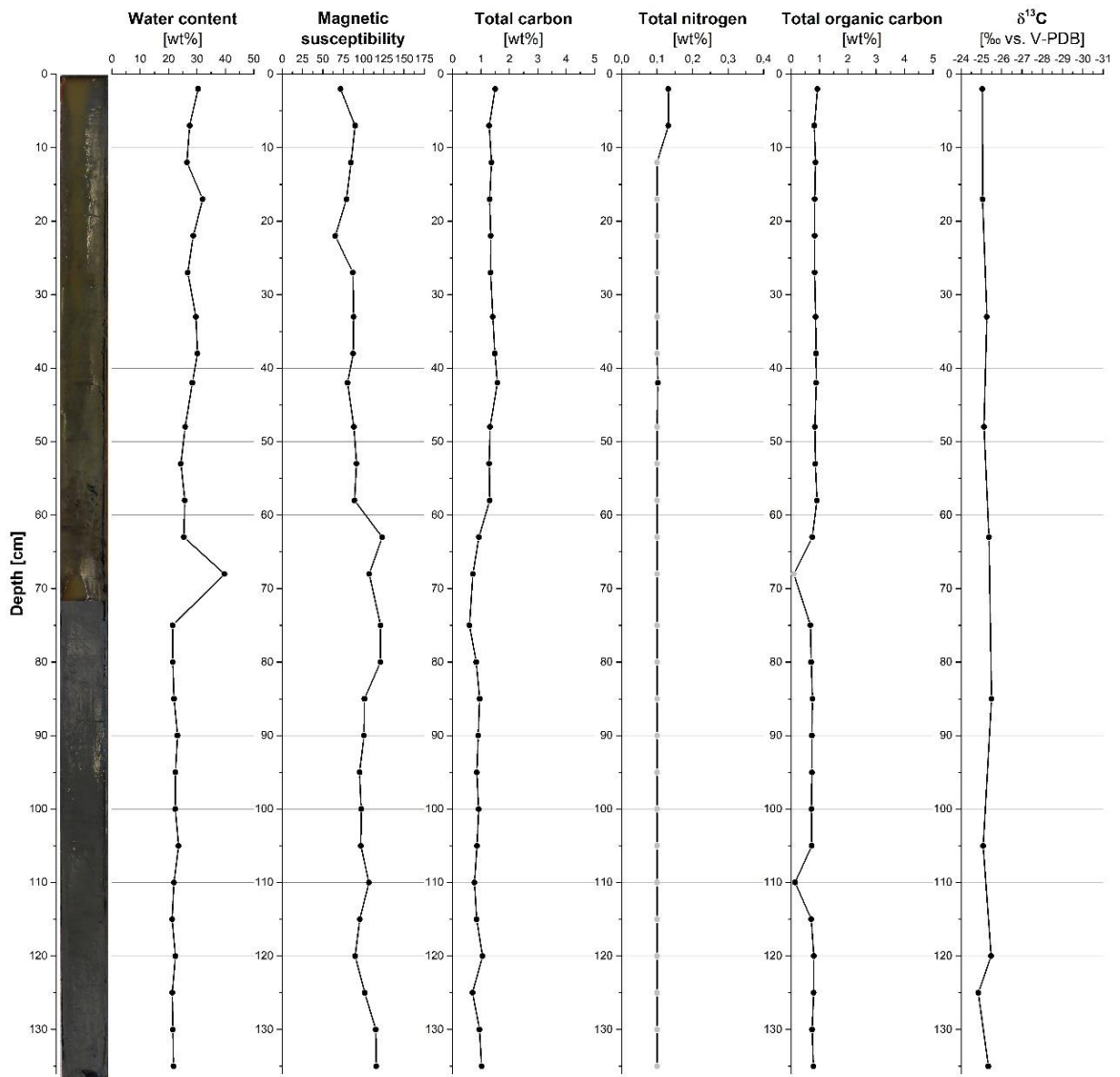
Figure 17: Core picture, water content, MS, TC, TN, TOC, δ13C of CAK17-GSL-T5-HC

5. Discussion

The sedimentary succession of all the cores can be interpreted as an archive of thermokarst lake development. Facies 1 represents sediment which was deposited within the recording lake evolution, whereas facies 2 represents a wetland peat describing the onset and initial lake development. Facies 3 can be interpreted as pre-lake sediment.

5.1 Lake internal depositional environment

Facies 1 is found in every core and describes the recording lake evolution. Hypothesis 1 is verified based on the following data interpretation:

Firstly, the magnetic susceptibility gives information about the availability of magnetic minerals and therefore indicates the input of inorganic allochthonous sediment into the lake (Thompson et al., 1975). The MS for facies 1 peaks at a) 140.90 in T1, b) 151.50 in T2, c) 117.20 in T3 and d) 123.20 in T5. The cores T1 that is close to the shore, show a higher maximum MS than the central core T3.

Secondly, a coarser grain size distribution is an indicator for a shorter transport path. Figure 18 shows the grains size distribution of the four cores. T1 shows a coarser grain size distribution with sandy silt and silt, while T3 shows a silt-rich distribution with a higher content of clay. T2 and T5 show a similar distribution like T1 but with a larger spread.

Thirdly, the origin of organic matter can be determined through the relation of δ^{13}C and the ratio of TOC and TN (Fig. 19). The δ^{13}C can be used to distinguish between marine and lacustrine algae, while the ratio of TOC and TN discerns between aquatic and terrestrial plants and can also be an organic matter degradation proxy. Facies 1 of near-shore core T1 shows wide ranging signals containing a mixture of lacustrine and some terrestrial organic matter, whereas T2 and T3 show a more centralized signal containing mostly lacustrine organic matter. T5 shows organic matter only from lacustrine origin. Altogether, near shore sediments contain a mixture of terrestrial and lacustrine organic matter while central lake sediments contain less organic matter from terrestrial origin.

The available data verifies hypothesis 1 clearly when comparing the core form near the shore T1 and the central lake core T3. Sediment core T2 and T5 show different patterns. The MS and the content of terrestrial organic matter do not decrease gradually from the near shore to the lake center. The data of the two cores between shore and center could be influenced by special events as thermokarst lakes tend to be very dynamic (Lenz et al., 2013, Biskaborn et al., 2013, Lenz et al., 2016b). Sediment core T2 shows an organic-rich

layer with low MS and high water content at 70 cm which is not present in the other cores. This could indicate such an event, where material is transported into the lake by shore expansion for example through outcropping ice wedges.
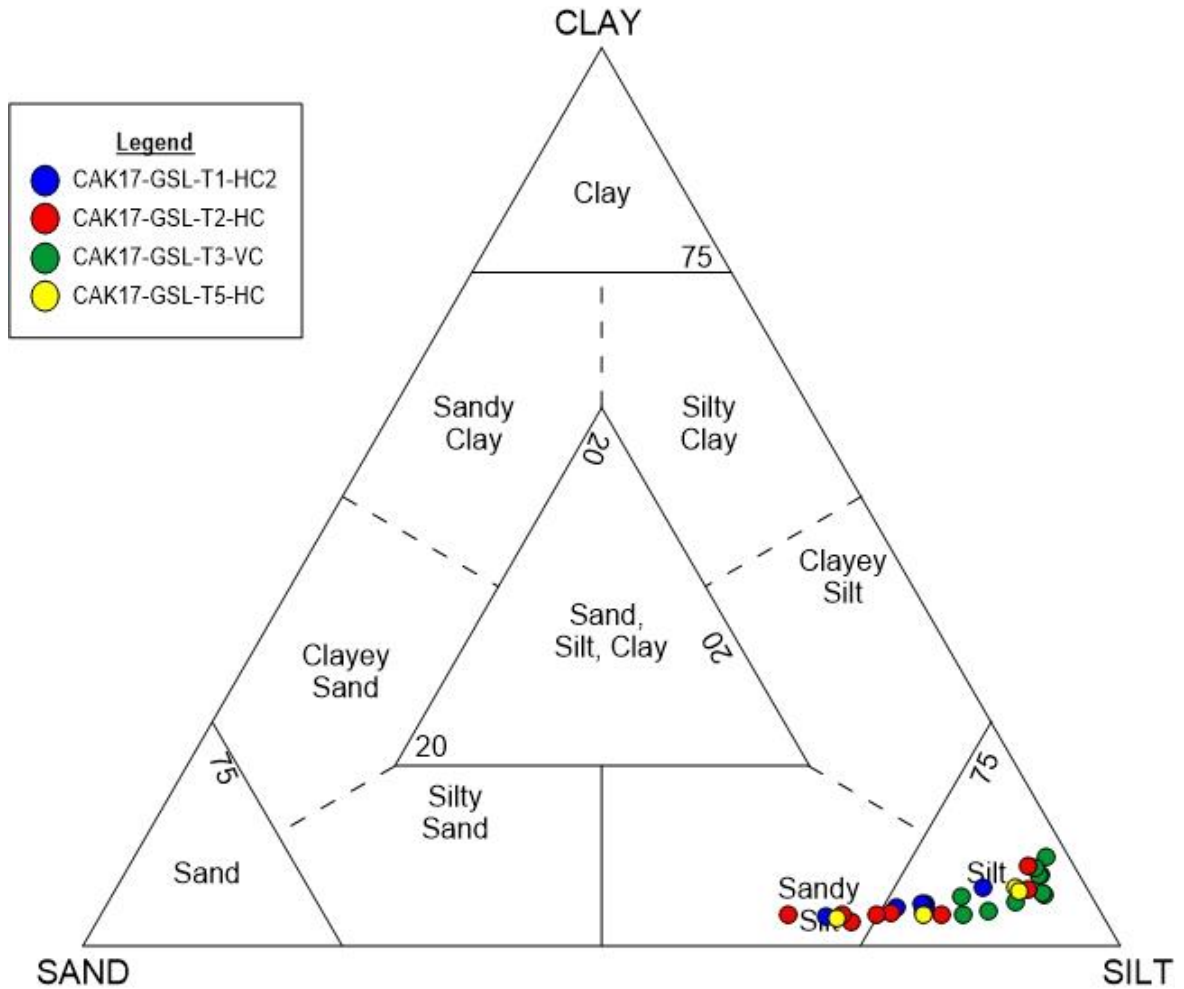
Figure 18: Grain size distribution of facies 1 in T1, T2, T3 and T5
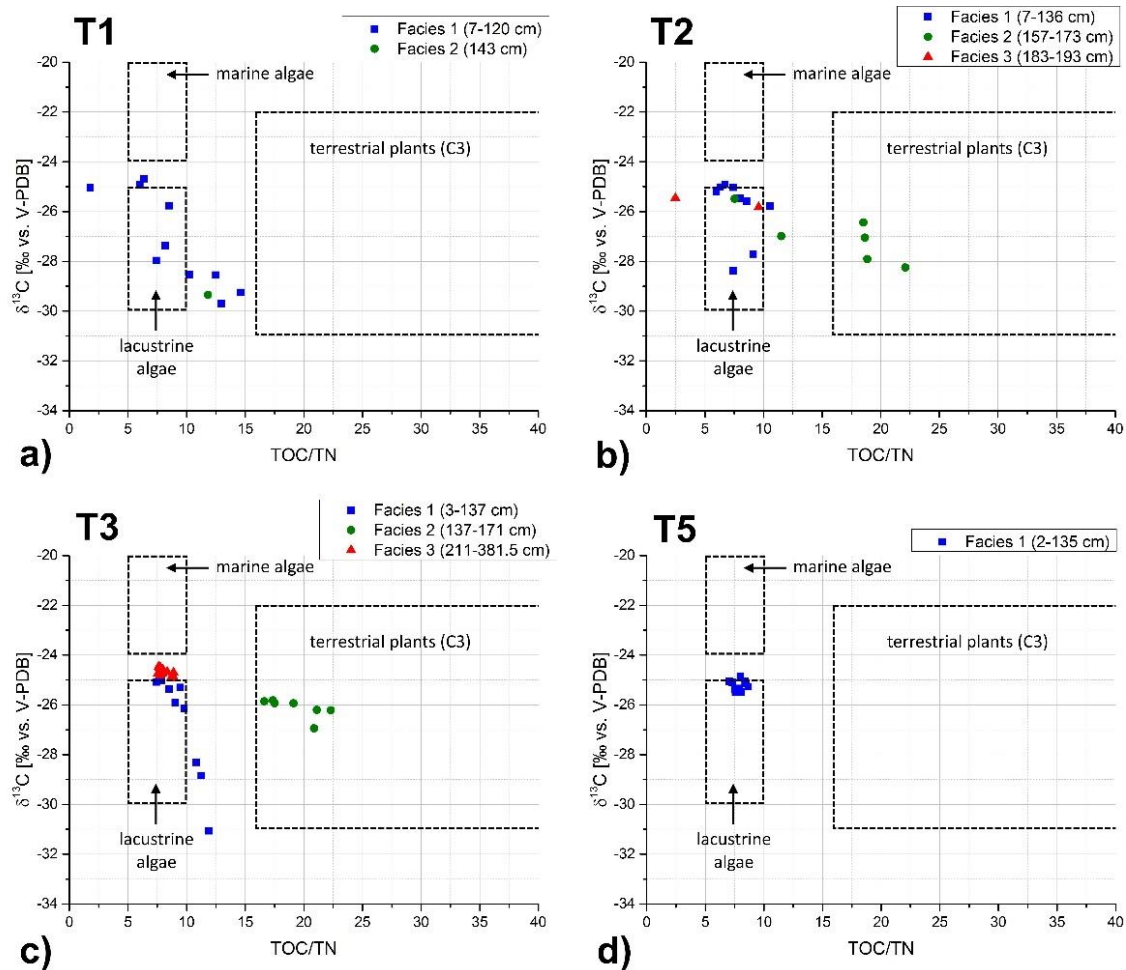
Figure 19: Ratio of δ¹³C and TOC/TN for the distinction between terrestrial plants and lacustrine/marine algae of Goldstream Lake cores a) T1, b) T2, c) T3 and d) T5 (according to (Meyers, 1994) and (Meyers and Lallier-Vergès, 1999), modified).

5.2 Thermokarst lake evolution

According to hypothesis 2, the longer and central lake core T3 and the shorter core T2 show three facies which could potentially preserve the evolution of the lake. Facies 1 represents the existing lacustrine phase, facies 2 indicates the lake onset with a terrestrial peat layer which should be rich in poorly decomposed organic matter, whereas facies 3 preserves pre-lake deposits which are indicated by terrestrial organic matter and a low TOC due to microbial decomposition.

Hypothesis 2 is partially verified and partially falsified based on the following data interpretation:

Firstly, facies 1 indicates a lacustrine environment as the origin of organic matter in T2 and T3 is dominated by lacustrine algae (blue squares Fig. 19 b and c). In addition, the water content and organic matter content is relatively low while the MS is high and variable, which indicates dynamic sediment deposition.

Secondly, in facies 2, the organic matter mainly originates from terrestrial plants (green circles in Fig. 19 b and c) and that the water and organic matter content reach their peaks, while the MS is at its lowest. This indicates a wetland peat layer and the onset of the lake. Thirdly, in facies 3, the water content is lower, and the MS shows similar high values like facies 1 but with a more regular pattern, which could indicate a less dynamic sediment input. The organic matter content is very low at the beginning of facies 3 and increases gradually to the end of the core. This can be explained as the microbial decomposition of organic matter is higher at the top as at the bottom.

According to hypothesis 2, facies 3 represents pre-lake sediments which should be dominated by terrestrial organic matter. Instead of terrestrial organic matter, facies 3 is dominated by lacustrine organic matter (red triangles in Fig. 19 b and c) which indicate a lacustrine depositional milieu. Therefore, the sediments of facies 3 could belong to an earlier lake generation. Therefore, Goldstream lake did not develop as a first-generation lake (Fig. 3) but rather followed a previous lake generation with an intermediate wetland as illustrated in figure 20. Marbled structures in facies 3 suggest cryoturbation occurring during the terrestrial phase where previous laminations were disturbed by newly formed permafrost.

In this scenario, a former lake generation experienced a drainage which would lead to the formation of a wetland. Due to the lost heat storage effect of the lake the talik froze which created new permafrost and led to cryoturbation of facies 3. The permafrost then thawed again and covered the wetland with excess water thus creating the present Goldstream Lake. Such dynamic geomorphologic changes of thermokarst lakes by drainage and refilling are very common in periglacial environments (Lenz et al., 2016c).

Hypothesis 2 is partially verified, since the longer sediment cores document the development of the lake and specifically the origin of facies 1 and 2 deposits. However, the origin of the organic matter and the development of facies 3 speak against terrestrial sediments and for the possible sediment record of a previous lake generation.
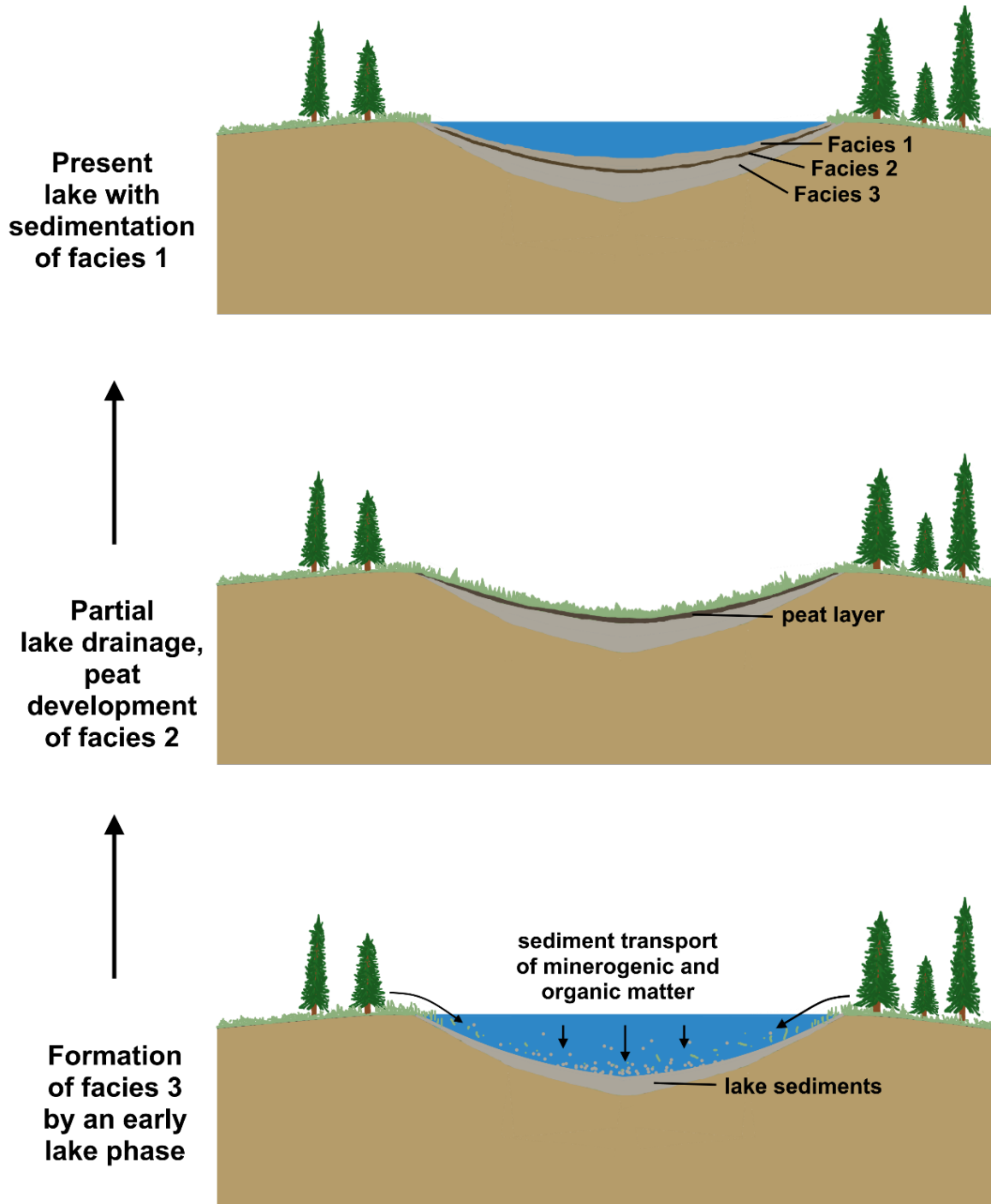
Figure 20: Simplified schematic evolution of Goldstream Lake

6. Conclusion and Outlook

This thesis dealt with the following hypotheses: 1) Near-shore deposits are characterized by a coarser grain size distribution, larger minerogenic input from terrestrial origin and a mixed source of lacustrine and terrestrial organic matter whereas central lake deposits are finer grained and contain less organic matter from terrestrial origin than near-shore sediments and, 2) a longer sediment record from the lake center potentially preserves pre-lake deposits which are indicated by terrestrial organic matter and low organic carbon content due to microbial decomposition in the talik. Low decomposed, terrestrial peat indicates the lake on-set and is followed by a lacustrine phase.

Near shore deposits are indeed characterized by a coarser grain size distribution, larger minerogenic input from terrestrial origin and a mixed source of lacustrine and terrestrial organic matter whereas central lake deposits are finer grained and contain less organic matter from terrestrial origin than near-shore sediments. The input event that occurred in T2 prove thermokarst lakes to be very dynamic systems. The used methods produce valuable data to study the lake internal depositional environment. Further cores from the western part of Goldstream Lake could allow a more detailed description of the depositional milieu, while other methods like the use of different bioindicators could support the organic matter origin results.

The longer cores preserve sediment of the present lake, a wetland peat and the sediments of a previous lake generation. The biogeochemical methods deliver excellent result by describing the evolution of Goldstream Lake perfectly. Even longer cores could indicate even older generations of thermokarst lakes and radiocarbon dating would provide important data on the age of the lake evolution stages. Further cores and the study of satellite images could also help to determine the position of the previous lake generation.

Overall, the methods and results provide a valuable insight into the internal deposition environment and the evolution of a thermokarst lake in discontinuous permafrost.

7. References

BARTINGTON-INSTRUMENTS 2017. Operation Manual for MS2 Magnetic Susceptibility System. Oxford, England: Bartington Instruments Limited.

BISKABORN, B. K., HERZSCHUH, U., BOLSHIYANOV, D. Y., SCHWAMBORN, G. & DIEKMANN, B. 2013. Thermokarst processes and depositional events in a tundra lake, northeastern Siberia. *Permafrost and Periglacial Processes,* 24**,** 160-174.

BROSIUS, L., WALTER ANTHONY, K., GROSSE, G., CHANTON, J., FARQUHARSON, L., OVERDUIN, P. P. & MEYER, H. 2012. Using the deuterium isotope composition of permafrost meltwater to constrain thermokarst lake contributions to atmospheric CH4 during the last deglaciation. *Journal of Geophysical Research: Biogeosciences,* 117.

ELSTER, J., LUKESOVÁ, A., SVOBODA, J., KOPECKY, J. & KANDA, H. 1999. Diversity and abundance of soil algae in the polar desert, Sverdrup Pass, central Ellesmere Island. *Polar Record,* 35**,** 231-254.

FRENCH, H. M. 2013. *The periglacial environment*, John Wiley & Sons.

JORGENSON, M., YOSHIKAWA, K., KANEVSKIY, M., SHUR, Y., ROMANOVSKY, V., MARCHENKO, S., GROSSE, G., BROWN, J. & JONES, B. Permafrost characteristics of Alaska. Proceedings of the Ninth International Conference on Permafrost, 2008. University of Alaska: Fairbanks, 121-122.

KESSLER, M., PLUG, L. J. & WALTER ANTHONY, K. 2012. Simulating the decadal-to millennial-scale dynamics of morphology and sequestered carbon mobilization of two thermokarst lakes in NW Alaska. *Journal of Geophysical Research: Biogeosciences,* 117.

LENZ, J., FRITZ, M., SCHIRRMEISTER, L., LANTUIT, H., WOOLLER, M. J., POLLARD, W. H. & WETTERICH, S. 2013. Periglacial landscape dynamics in the western Canadian Arctic: results from a thermokarst lake record on a push moraine (Herschel Island, Yukon Territory). *Palaeogeography, Palaeoclimatology, Palaeoecology,* 381**,** 15-25.

LENZ, J., GROSSE, G., JONES, B. M., ANTHONY, W., KATEY, M., BOBROV, A., WULF, S. & WETTERICH, S. 2016a. Mid-Wisconsin to Holocene Permafrost and Landscape Dynamics based on a Drained Lake Basin Core from the Northern Seward Peninsula, Northwest Alaska. *Permafrost and Periglacial Processes,* 27**,** 56-75.

LENZ, J., JONES, B. M., WETTERICH, S., TJALLINGII, R., FRITZ, M., ARP, C. D., RUDAYA, N. & GROSSE, G. 2016b. Impacts of shore expansion and catchment characteristics on lacustrine thermokarst records in permafrost lowlands, Alaska Arctic Coastal Plain. *arktos,* 2**,** 25.

LENZ, J., WETTERICH, S., JONES, B. M., MEYER, H., BOBROV, A. & GROSSE, G. 2016c. Evidence of multiple thermokarst lake generations from an 11 800-year-old permafrost core on the northern Seward Peninsula, Alaska. *Boreas,* 45**,** 584-603.

LEONHARD, K. V. 1823. Charakteristik der Felsarten, 3 vols. Engelmann Verlag Heidelberg.

MEYERS, P. A. 1994. Preservation of elemental and isotopic source identification of sedimentary organic matter. *Chemical Geology,* 114**,** 289-302.

MEYERS, P. A. & LALLIER-VERGÈS, E. 1999. Lacustrine sedimentary organic matter records of Late Quaternary paleoclimates. *Journal of Paleolimnology,* 21**,** 345-372.

MUNSELL, A. H. 2013. *Munsell Soil Color Charts: With Genuine Munsell* Color Chips*, Munsell Color.

OSTERKAMP, T. 2005. The recent warming of permafrost in Alaska. *Global and Planetary Change,* 49**,** 187-202.

PETRENKO, V. V., SMITH, A. M., BROOK, E. J., LOWE, D., RIEDEL, K., BRAILSFORD, G., HUA, Q., SCHAEFER, H., REEH, N. & WEISS, R. F. 2009. 14CH4 measurements in Greenland ice: investigating last glacial termination CH4 sources. *Science,* 324**,** 506-508.

PÉWÉ, T. L. 1975. *Quaternary geology of Alaska*, US Government Printing Office.

RAUTIO, M. & VINCENT, W. F. 2006. Benthic and pelagic food resources for zooplankton in shallow high-latitude lakes and ponds. *Freshwater Biology,* 51**,** 1038-1052.

SCHIRRMEISTER, L., GROSSE, G., WETTERICH, S., OVERDUIN, P. P., STRAUSS, J., SCHUUR, E. A. & HUBBERTEN, H. W. 2011. Fossil organic matter characteristics in permafrost deposits of the northeast Siberian Arctic. *Journal of Geophysical Research: Biogeosciences,* 116.

STOCKER, T. 2014. *Climate change 2013: the physical science basis: Working Group I contribution to the Fifth assessment report of the Intergovernmental Panel on Climate Change*, Cambridge University Press.

STRAUSS, J., SCHIRRMEISTER, L., GROSSE, G., FORTIER, D., HUGELIUS, G., KNOBLAUCH, C., ROMANOVSKY, V., SCHÄDEL, C., VON DEIMLING, T. S. & SCHUUR, E. A. 2017. Deep Yedoma permafrost: A synthesis of depositional characteristics and carbon vulnerability. *Earth-Science Reviews,* 172**,** 75-86.

STRAUSS, J., SCHIRRMEISTER, L., GROSSE, G., WETTERICH, S., ULRICH, M., HERZSCHUH, U. & HUBBERTEN, H. W. 2013. The deep permafrost carbon pool of the Yedoma region in Siberia and Alaska. *Geophysical Research Letters,* 40**,** 6165-6170.

THOMPSON, R., BATTARBEE, R. W., O'SULLIVAN, P. & OLDFIELD, F. 1975. Magnetic susceptibility of lake sediments. *Limnology and Oceanography,* 20**,** 687-698.

VAN EVERDINGEN, R. 2005. Multi-language glossary of permafrost and related ground-ice terms, National Snow and Ice Data Center/World Data Center for Glaciology, Boulder. *World Wide Web Address:* http://nsidc. *org/fgdc/glossary*.

VÉZINA, S. & VINCENT, W. F. 1997. Arctic cyanobacteria and limnological properties of their environment: Bylot Island, Northwest Territories, Canada (73 N, 80 W). *Polar Biology,* 17**,** 523-534.

VIERECK, L. A., DYRNESS, C., BATTEN, A. & WENZLICK, K. 1992. The Alaska vegetation classification.

WALTER ANTHONY, K. M., ZIMOV, S. A., GROSSE, G., JONES, M. C., ANTHONY, P. M., III, F. S. C., FINLAY, J. C., MACK, M. C., DAVYDOV, S., FRENZEL, P. & FROLKING, S. 2014. A shift of thermokarst lakes from carbon sources to sinks during the Holocene epoch. *Nature,* 511**,** 452-456.

WALTER, K., EDWARDS, M., GROSSE, G., ZIMOV, S. & CHAPIN, F. 2007. Thermokarst lakes as a source of atmospheric CH 4 during the last deglaciation. *science,* 318**,** 633-636.

WALTER, K. M., ZIMOV, S., CHANTON, J. P., VERBYLA, D. & CHAPIN, F. S. 2006. Methane bubbling from Siberian thaw lakes as a positive feedback to climate warming. *Nature,* 443**,** 71-75.

ZHANG, T., BARRY, R. G., KNOWLES, K., HEGINBOTTOM, J. A. & BROWN, J. 1999. Statistics and characteristics of permafrost and ground-ice distribution in the Northern Hemisphere. *Polar Geography,* 23**,** 132-154.

ZHANG, T., HEGINBOTTOM, J. A., BARRY, R. G. & BROWN, J. 2000. Further statistics on the distribution of permafrost and ground ice in the Northern Hemisphere. *Polar Geography,* 24**,** 126-131.

8. Appendix

Table 2: Water depth data of Goldstream Lake

Lat (°)	long (°)	depth (m)	Date of measurement
64,91566	147,8479	2,70	05.11.12
64,9157	147,84732	2,50	05.02.12
64,91566	147,8479	2,80	05.08.12
64,91576	-147,8473	1,50	03.28.12
64,91565	147,8479	2,85	04.19.12
64,91565	-147,8479	2,47	03.08.12
64,91576	-147,8473	1,70	03.08.12
64,91566	-147,8479	2,40	07.11.11
64,91567	-147,8474	2,50	07.11.11
64,91596	-147,84749	1,96	05.09.11
64,91594	-147,84749	2,12	05.09.11
64,91593	-147,8474	2,03	05.03.11
64,91569	-147,84822	2,33	04.13.11
64,91596	-147,84749	1,72	04.13.11
	mean	1,9	Aug 2013
	max	3,3	Aug 2013

Table 3: Sampling range, depth, water content, MS, TN, TC, TOC of CAK17-GSL-T1-HC2

Sampling range (cm)	Depth (cm)	water content (%)	MS-LF	N (%)	C (%)	TOC (%)
1,5-2,5	2,0	62,6630	32,40	0,345	4,844	3,934
6,5-7,5	7,0	57,1946	40,15	0,303	4,869	3,915
11,5-12,5	12,0	47,0088	52,30	0,193	3,585	2,823
16,5-17,5	17,0	43,8191	60,70	0,141	2,665	1,950
21,5-22,5	22,0	43,9129	69,05	0,164	2,704	2,044
27,5-28,5	28,0	33,2051	93,57	< 0,10	1,685	1,239
34,5-35,5	35,0	33,9438	110,10	< 0,10	1,527	1,023
39,5-40,5	40,0	33,2995	92,07	0,121	1,713	1,127
44,5-45,5	45,0	31,8765	93,53	0,164	1,526	1,213
49,5-50,5	50,0	33,3301	96,63	< 0,10	1,756	1,332
54,5-55,5	55,0	34,4143	87,65	0,180	1,665	1,471
59,5-60,5	60,0	31,0609	96,27	0,170	1,803	1,629
64,5-65,5	65,0	23,1106	116,80	0,126	1,230	1,075
69,5-70,5	70,0	24,5238	87,40	0,156	1,718	1,605
74,5-75,5	75,0	21,6070	120,13	< 0,10	0,897	0,760
79,5-80,5	80,0	21,0218	140,90	< 0,10	0,803	<0,10
84,5-85,5	85,0	21,0350	134,25	0,102	0,876	0,182
89,5-90,5	90,0	21,7891	133,57	0,106	0,949	0,747
94,5-95,5	95,0	36,7252	131,63	0,126	1,097	0,773
99,5-100,5	100,0	23,2533	103,63	0,122	1,090	0,776
104,5-105,5	105,0	22,6198	129,63	0,134	1,063	0,779
109,5-110,5	110,0	21,5971	134,07	0,124	0,972	0,765
114,5-115,5	115,0	23,0406	93,50	0,134	1,121	0,791
119,5-120,5	120,0	22,1046	125,27	0,132	1,129	0,794
124,5-125,5	125,0	23,6659	106,27	0,148	1,212	0,825
129,5-130,5	130,0	25,8888	93,60	0,194	1,508	1,027
134,5-135,5	135,0	25,8824	93,05	0,192	1,535	1,060
139,5-140,5	140,0	25,8844	85,20	0,200	1,585	1,087
142,5-143,5	143,0	47,5665	57,00	0,311	4,136	3,670

Table 4: Sampling range, depth, water content, MS, TN, TC, TOC of CAK17-GSL-T2-HC

Sampling range (cm)	Depth (cm)	water content (%)	MS-LF	N (%)	C (%)	TOC (%)
1,5-2,5	2,0	24,0440	122,30	0,123	0,974	0,789
6,5-7,5	7,0	23,5242	119,50	0,114	0,938	0,763
11,5-12,5	12,0	25,6383	112,83	0,122	1,014	0,817
16,5-17,5	17,0	25,1131	117,73	0,105	0,932	0,773
21,5-22,5	22,0	23,2174	124,23	0,102	0,855	0,771
29,5-30,5	30,0	25,3784	125,75	0,129	1,104	0,815
45,5-46,5	46,0	29,3908	83,17	0,159	1,450	0,952
50,5-51,5	51,0	35,8842	67,77	0,214	1,669	1,347
55,5-56,5	56,0	23,7000	102,30	< 0,10	0,749	0,594
60,5-61,5	61,0	23,2012	97,43	< 0,10	0,730	0,438
66,5-67,5	67,0	47,1122	34,15	0,358	2,900	2,646
70,5-71,5	71,0	58,4532	19,93	0,577	5,811	5,568
74,5-75,5	75,0	46,6191	16,43	0,348	3,374	3,172
80,5-81,5	81,0	21,6938	107,27	< 0,10	0,805	0,800
85,5-86,5	86,0	23,3616	137,87	0,120	1,421	1,269
90,5-91,5	91,0	21,5275	151,50	< 0,10	0,880	0,810
95,5-96,5	96,0	21,8655	131,13	< 0,10	1,114	0,942
100,5-101,5	101,0	22,3772	94,27	0,121	1,194	0,968
105,5-106,5	106,0	22,7454	100,30	0,112265	1,12978047	0,943
110,5-111,5	111,0	22,2349	126,53	0,10224898	1,114	0,875
115,5-116,5	116,0	21,6980	124,10	< 0,10	0,816	0,740
120,5-121,5	121,0	22,6131	116,07	< 0,10	0,831	0,750
125,5-126,5	126,0	26,6360	92,87	< 0,10	0,868	0,783
129,5-130,5	130,0	22,3941	100,80	< 0,10	0,861	0,803
135,5-136,5	136,0	23,5634	88,80	< 0,10	0,922	0,798
140,5-141,5	141,0	23,4890	100,90	< 0,10	0,870	0,783
145,5-146,5	146,0	22,7323	108,20	< 0,10	0,750	0,716
151,5-152,5	152,0	25,1019	112,13	< 0,10	0,944	0,799
156,5-157,5	157,0	42,0684	52,87	0,243	4,697	4,587
158,5-159,5	159,0	52,1831	36,70	0,354	7,819	7,822
160,5-161,5	161,0	28,9215	90,83	0,126	1,835	1,448
163,5-164,5	164,0	44,5476	55,70	0,369	7,033	6,821
168,5-169,5	169,0	23,1923	108,40	< 0,10	0,847	0,754
172,5-173,5	173,0	26,8049	84,10	0,115	2,557	2,143
177,5-178,5	178,0	21,4966	114,67	< 0,10	0,989	0,850
182,5-183,5	183,0	20,2247	147,85	< 0,10	0,799	0,248
187,5-188,5	188,0	20,6001	170,87	< 0,10	0,950	0,821
192,5-193,5	193,0	20,3042	84,47	< 0,10	1,119	0,959
197,5-198,5	198,0	19,3086	79,33	< 0,10	1,068	0,929
202,5-203,5	203,0	30,6423	71,10	0,119	1,716	1,436

Table 5: Sampling range, depth, water content, MS, TN, TC, TOC of CAK17-GSL-T3-VC

Sampling range (cm)	Depth (cm)	water content (%)	MS-LF	N (%)	C (%)	TOC (%)
0,5-1,5	1,0	36,5972	56,70	0,157	2,113	1,475
5,5-6,5	6,0	33,6037	62,35	0,154	2,173	1,374
10,5-11,5	11,0	27,1058	91,20	< 0,10	1,019	0,799
2,5-3,5	3,0	33,6348	69,25	0,132	1,881	1,242
15,5-16,5	16,0	26,4087	96,93	< 0,10	1,045	0,817
20,5-21,5	21,0	28,6276	80,00	0,116	1,596	1,068
25,5-26,5	26,0	26,7147	84,00	< 0,10	1,117	0,803
30,5-31,5	31,0	28,9076	77,17	< 0,10	1,475	0,941
35,5-36,5	36,0	24,9304	95,75	< 0,10	0,908	0,742
40,5-41,5	41,0	25,0643	110,45	< 0,10	0,876	0,728
45,5-46,5	46,0	26,3532	78,43	< 0,10	1,395	0,901
50,5-51,5	51,0	26,1656	96,60	< 0,10	0,893	0,740
56,5-57,5	57,0	28,7399	89,10	< 0,10	1,270	0,979
61,5-62,5	62,0	24,9219	104,40	< 0,10	0,890	0,746
69,5-70,5	70,0	28,6287	94,93	< 0,10	1,164	0,903
74,5-75,5	75,0	25,8046	96,27	< 0,10	1,062	0,767
79,5-80,5	80,0	28,0890	117,20	< 0,10	0,766	0,779
84,5-85,5	85,0	25,3413	91,30	< 0,10	1,109	0,785
89,5-90,5	90,0	24,2685	106,07	< 0,10	0,781	< 0,10
95,5-96,5	96,0	23,6858	115,30	< 0,10	0,695	< 0,10
101,5-102,5	102,0	30,7430	70,55	< 0,10	1,555	0,982
106,5-107,5	107,0	26,3079	79,40	< 0,10	1,183	0,836
111,5-112,5	112,0	26,9450	78,97	< 0,10	1,183	0,852
114,5-115,5	115,0	38,1659	58,07	0,232	2,787	2,327
120,5-121,5	121,0	54,2194	31,15	0,592	7,031	7,033
117,5-118,5	118,0	26,0222	81,13	0,107	1,321	1,026
125,5-126,5	126,0	23,8395	100,27	< 0,10	0,840	0,755
129-130	129,5	37,4706	52,50	0,232	2,794	2,505
132,5-133,5	133,0	29,8447	63,65	0,142	1,949	1,684
136,5-137,5	137,0	40,4478	44,63	0,307	3,677	3,459
141,5-142,5	142,0	65,9052	9,70	0,839	17,823	17,514
146,5-147,5	147,0	69,1826	6,85	1,302	28,348	29,031
150,5-151,5	151,0	38,9469	22,30	0,332	6,791	7,004
155,5-156,5	156,0	24,8740	32,00	0,181	3,438	3,460
160,5-161,5	161,0	23,2517	55,30	0,165	2,845	2,735
165,5-166,5	166,0	21,2140	66,15	0,129	2,347	2,232
170,5-171,5	171,0	19,6204	54,55	< 0,10	1,938	1,751
175,5-176,5	176,0	16,3350	120,07	< 0,10	0,654	0,745
180,5-181,5	181,0	16,5800	126,97	< 0,10	0,502	< 0,10
185,5-186,5	186,0	15,9386	130,90	< 0,10	0,521	< 0,10
190,5-191,5	191,0	16,4686	131,10			
195,5-196,5	196,0	19,0354	98,35	< 0,10	0,976	< 0,10
200,5-201,5	201,0	19,2481	87,90	< 0,10	0,973	< 0,10
205,5-206,5	206,0	18,0108	107,05	< 0,10	1,035	< 0,10
211-212	211,5	18,9264	97,33	< 0,10	1,032	0,756
215,5-216,5	216,0	18,9305	93,65	< 0,10	1,039	0,1
220,5-221,5	221,0	20,0598	90,35	< 0,10	1,212	0,794
225,5-226,5	226,0	21,2385	98,10	0,116	1,360	0,918
231-232	231,5	21,1350	95,85	0,128	1,479	0,988
234,5-235,5	235,0	22,6856	98,05	0,115	1,418	0,873
239,5-240,5	240,0	22,4008	92,75	0,104	1,359	0,854
244,5-245,5	245,0	21,2288	94,75	< 0,10	1,255	0,805

249,5-250,5	250,0	21,3537	97,90	< 0,10	1,180	0,798
254,5-255,5	255,0	22,3604	89,80	0,104	1,260	0,828
259,5-260,5	260,0	21,9435	95,70	< 0,10	1,304	0,831
264,5-265,5	265,0	22,7324	89,55	0,104	1,346	0,864
269,5-270,5	270,0	22,0455	96,65	0,105	1,278	0,807
274,5-275,5	275,0	21,7971	92,05	< 0,10	1,366	0,793
279,5-280,5	280,0	21,7650	95,75	< 0,10	1,272	0,771
284,5-285,5	285,0	22,6530	90,25	< 0,10	1,320	0,803
289,5-290,5	290,0	22,2148	95,80	< 0,10	1,279	0,791
294,5-295,5	295,0	22,9141	92,05	< 0,10	1,341	0,779
299,5-300,5	300,0	22,7199	93,80	< 0,10	1,294	0,792
304,5-305,5	305,0	23,8591	85,60	< 0,10	1,465	0,888
309,5-310,5	310,0	25,8436	81,25	0,158	1,956	1,386
314,5-315,5	315,0	26,5300	77,95	0,183	2,263	1,630
319,5-320,5	320,0	27,4281	78,05	0,197	2,498	1,843
324,5-325,5	325,0	27,7168	69,35	0,214	2,566	1,857
329,5-330,5	330,0	28,2137	62,60	0,172	2,709	1,768
334,5-335,5	335,0	27,6577	55,75	0,163	2,517	1,759
339,5-340,5	340,0	30,8710	58,95	0,213	3,417	2,255
344,5-345,5	345,0	24,9002	78,00	0,177	1,938	1,135
349,5-350,5	350,0	21,2839	105,05	< 0,10	1,398	0,873
354,5-355,5	355,0	23,2830	83,95	0,135	1,82	1,347
359,5-360,5	360,0	25,1636	89,80	0,188	2,074	1,655
364,5-365,5	365,0	33,2172	69,60	0,289	3,007	2,732
369,5-370,5	370,0	27,2149	82,05	0,216	2,487	2,114
373,5-374,5	374,0	21,7209	110,45	0,112	1,373	1,078
377,5-378,5	378,0	22,8957	98,40	0,137	1,654	1,378
381-382	381,5	20,7705	93,05	0,143	1,88	1,610

Table 6: Sampling range, depth, water content, MS, TN, TC, TOC of CAK17-GSL-T5-HC

Sampling range (cm)	Depth (cm)	water content (%)	MS-LF	N (%)	C(%)	TOC(%)
1.25-2.75	2,0	30,3746	71,80	0,132	1,499	0,933
6,25-7,75	7,0	27,4326	89,73	0,132	1,292	0,823
11,25-12,75	12,0	26,4774	84,70	< 0,10	1,372	0,862
16,5-17,5	17,0	31,9909	79,25	< 0,10	1,307	0,840
21,5-22,5	22,0	28,6855	65,40	< 0,10	1,346	0,836
26,5-27,5	27,0	26,7663	87,00	< 0,10	1,343	0,835
32,5-33,5	33,0	29,6088	87,90	< 0,10	1,421	0,867
37,5-38,5	38,0	30,1586	87,47	< 0,10	1,491	0,885
41,5-42,5	42,0	28,3989	80,50	0,102	1,580	0,889
47,5-48,5	48,0	25,8460	88,27	< 0,10	1,326	0,846
52,5-53,5	53,0	24,3350	91,50	< 0,10	1,292	0,857
57,5-58,5	58,0	25,7027	89,07	< 0,10	1,311	0,915
62,5-63,5	63,0	25,3797	123,20	< 0,10	0,930	0,751
67,5-68,5	68,0	39,6673	107,20	< 0,10	0,718	< 0,10
74,5-75,5	75,0	21,4491	121,17	< 0,10	0,596	0,688
79,5-80,5	80,0	21,4949	120,93	< 0,10	0,833	0,714
84,5-85,5	85,0	21,9251	101,33	< 0,10	0,953	0,758
89,5-90,5	90,0	23,1678	100,80	< 0,10	0,904	0,738
94,5-95,5	95,0	22,3916	95,33	< 0,10	0,856	0,738
99,5-100,5	100,0	22,3665	97,33	< 0,10	0,918	0,722
104,5-105,5	105,0	23,5185	96,90	< 0,10	0,862	0,729
109,5-110,5	110,0	21,8892	106,80	< 0,10	0,774	0,146
114,5-115,5	115,0	21,2609	95,53	< 0,10	0,848	0,714
119,5-120,5	120,0	22,4156	89,87	< 0,10	1,055	0,807
124,5-125,5	125,0	21,3182	101,75	< 0,10	0,705	0,8
129,5-130,5	130,0	21,5018	115,27	< 0,10	0,950	0,747
134,5-135,5	135,0	21,7299	115,95	< 0,10	1,020	0,792

Table 7: δ¹³C for all core

Sample ID		$\delta^{13}C$ (‰) vs. PDB		Sample ID		$\delta^{13}C$ (‰) vs. PDB
CAK17-GSL_T2-HC_	7cm	-24,91		CAK17-GSL-T3-VC_	70cm	-25,91
CAK17-GSL_T2-HC_	17cm	-25,03		CAK17-GSL-T3-VC_	112cm	-25,36
CAK17-GSL_T2-HC_	30cm	-25,02		CAK17-GSL-T3-VC_	121cm	-31,06
CAK17-GSL_T2-HC_	30cm*	-25,04		CAK17-GSL-T3-VC_	129,5cm	-28,31
CAK17-GSL_T2-HC_	46cm	-25,21		CAK17-GSL-T3-VC_	137cm	-28,84
CAK17-GSL_T2-HC_	67cm	-28,38		CAK17-GSL-T3-VC_	142cm	-26,94
CAK17-GSL_T2-HC_	75cm	-27,71		CAK17-GSL-T3-VC_	147cm	-26,22
CAK17-GSL_T2-HC_	86cm	-25,78		CAK17-GSL-T3-VC_	151cm	-26,20
CAK17-GSL_T2-HC_	111cm	-25,59		CAK17-GSL-T3-VC_	156cm	-25,94
CAK17-GSL_T2-HC_	136cm	-25,47		CAK17-GSL-T3-VC_	156cm*	-25,91
CAK17-GSL_T2-HC_	157cm	-27,91		CAK17-GSL-T3-VC_	171cm	-25,93
CAK17-GSL_T2-HC_	159cm	-28,25		CAK17-GSL-T3-VC_	221cm	-24,74
CAK17-GSL_T2-HC_	159cm*	-28,29		CAK17-GSL-T3-VC_	231,5cm	-24,81
CAK17-GSL_T2-HC_	161cm	-26,99		CAK17-GSL-T3-VC_	235 cm	-24,46
CAK17-GSL_T2-HC_	164cm	-26,44		CAK17-GSL-T3-VC_	250cm	-24,58
CAK17-GSL_T2-HC_	169cm	-25,49		CAK17-GSL-T3-VC_	265cm	-24,67
CAK17-GSL_T2-HC_	173cm	-27,05		CAK17-GSL-T3-VC_	280cm	-24,49
CAK17-GSL_T2-HC_	183cm	-25,46		CAK17-GSL-T3-VC_	295cm	-24,52
CAK17-GSL_T2-HC_	183cm*	-25,44		CAK17-GSL-T3-VC_	305cm	-24,70
CAK17-GSL_T2-HC_	193cm	-25,82		CAK17-GSL-T3-VC_	305cm*	-24,72
CAK17-GSL-T1-HC2_	7cm	-29,69		CAK17-GSL-T3-VC_	315cm	-24,89
CAK17-GSL-T1-HC2_	12cm	-29,25		CAK17-GSL-T3-VC_	325cm	-24,92
CAK17-GSL-T1-HC2_	22cm	-28,55		CAK17-GSL-T3-VC_	335cm	-24,82
CAK17-GSL-T1-HC2_	35cm	-28,53		CAK17-GSL-T3-VC_	350cm	-24,52
CAK17-GSL-T1-HC2_	45cm	-27,97		CAK17-GSL-T3-VC_	365cm	-25,13
CAK17-GSL-T1-HC2_	55cm	-27,37		CAK17-GSL-T3-VC_	381.5cm	-24,87
CAK17-GSL-T1-HC2_	55cm*	-27,44		CAK17-GSL-T5-HC_	2cm	-25,05
CAK17-GSL-T1-HC2_	65cm	-25,77		CAK17-GSL-T5-HC_	17cm	-25,06
CAK17-GSL-T1-HC2_	85cm	-25,05		CAK17-GSL-T5-HC_	33cm	-25,27
CAK17-GSL-T1-HC2_	85cm*	-25,03		CAK17-GSL-T5-HC_	33cm*	-25,21
CAK17-GSL-T1-HC2_	100cm	-24,68		CAK17-GSL-T5-HC_	48cm	-25,13
CAK17-GSL-T1-HC2_	120cm	-24,92		CAK17-GSL-T5-HC_	63cm	-25,37
CAK17-GSL-T1-HC2_	143cm	-29,35		CAK17-GSL-T5-HC_	85cm	-25,50
CAK17-GSL-T3-V3_	85cm	-25,01		CAK17-GSL-T5-HC_	105cm	-25,09
CAK17-GSL-T3-V3_	85cm*	-25,07		CAK17-GSL-T5-HC_	120cm	-25,48
CAK17-GSL-T3-V3_	161cm	-25,86		CAK17-GSL-T5-HC_	125cm	-24,85
CAK17-GSL-T3-V3_	166cm	-25,82		CAK17-GSL-T5-HC_	135cm	-25,34
CAK17-GSL-T3-V3_	211cm	-24,70				
CAK17-GSL-T3-VC_	3cm	-25,30				
CAK17-GSL-T3-VC_	3cm*	-25,26				
CAK17-GSL-T3-VC_	36cm	-25,08				
CAK17-GSL-T3-VC_	57cm	-26,14				